A NEW TWO-DIMENSIONAL BLOOD FLOW MODEL AND ITS RKDG APPROXIMATION

Mehmet Ersoy, Yolhan Mannes, Omer Eker

A NEW TWO-DIMENSIONAL BLOOD FLOW MODEL AND ITS RKDG APPROXIMATION

Y. MANNES, M. ERSOY, AND O.F. EKER

Abstract. We propose a new two-dimensional blood flow reduced model taking into account of complex artery geometry as in the case of severe aneurysm. We derive the model from the three-dimensional Navier–Stokes equations written in a curvilinear coordinate system under the thin-artery assumption, with boundary conditions including wall tissue deformation. We show that the model is energetically consistent with the full Navier-Stokes problem. This model, obtained via radial averaging, is, up to our knowledge, the first one. It has the advantage of being more accurate than the classical one-dimensional models and to be solved in a reasonable time in comparison with the Navier-Stokes models. To this purpose, we use a Runge Kutta Discontinuous Galerkin (RKDG) method to solve the two-dimensional problem. We end the paper with several numerical test cases to show the efficiency and robustness of the numerical model, and in particular, we show the limit of the one-dimensional models in the case of a severe aneurysm.

Contents

1. Introduction

Modeling the cardiovascular system in arteries holds a central place in medical science, particularly in connection with cardiovascular diseases such as coronary heart disease, stroke, peripheral artery disease, aneurysms, and among others. This is especially important today in understanding and forecasting the impact of developed countries' way of life on people's healthcare (around 30%

Date: September 17, 2024.
Key words and phrases. Blood Flow, Asymptotic Analysis, Thin-Artery Assumption, Energy Consistency, RKDG Method, Aneurysm.

of cardiovascular disease deaths are from developed countries). Therefore, it is of major interest to develop an accurate mathematical model.

The dynamic of such flow is mainly influenced by the fluid-structure interaction with the artery wall. The forecast to predict the motion of blood through the artery is a difficult task to which substantial effort has been devoted [12, 11, 4, 3, 2, 19, 20, 17].

One of the most widely used models to describe the motion of blood through the artery is the one-dimensional (1D) Blood Flow equation derived, for instance, in [1, 18, 2, 19, 12, 16]. This classical model is a hyperbolic system of Partial Differential Equations (PDE) describing the conservation laws linking the wall elasticity to the fluid dynamics. This model is derived from an ansatz for the velocity profile in Eq. (2) and reads,

$$\left\{\begin{array}{rcl} \partial_t A + \partial_x Q & = & 0, \\ \partial_t Q + \partial_x(\alpha\frac{Q^2}{A} + \frac{1}{\rho}AP(A,x)) & = & \frac{1}{\rho}P(A,x)\partial_x A - K\frac{Q}{A}, \end{array}\right. \tag{1}$$

where the unknowns $A(t,x)$ stands artery's section area (assumed to be cylindrical), $Q(t,x) = A(t,x)\overline{u_x}(t,x)$ is the flow rate and $\overline{u_x}$ is the mean speed over the artery's section (see [19, 12] for further details). The function $P(A,x)$ denotes the pressure of blood at the wall and reads,

$$P(A,x) = b(x)\frac{\sqrt{A}-\sqrt{A_0}}{A_0},$$

where b encompasses the elastic behavior of the artery, *i.e.*, $b(x) = \frac{E(x)}{1-\xi}h\sqrt{\pi}$, where E is the Young's modulus, ξ is the Poisson ratio, and h is the wall thickness. The velocity profile is given by

$$u_x(t,r,x) = \frac{Q(t,x)}{A(t,x)}\frac{\gamma+2}{\gamma}\left[1-\left(\frac{r}{R(t,x)}\right)^\gamma\right], \tag{2}$$

where γ is an integer (often set to 9, see for instance [19, 13]). The friction term K is defined as a function of γ by $K = 2\pi\nu(\gamma+2)$ where ν is the kinematic viscosity of the blood. In Eq. (1), the Bousinessq coefficient is given by $\alpha = \frac{\gamma+2}{\gamma+1}$ (*c.f.*[19, 13, 20]). In recent work, [**?**] inspired from [8, 10, 14], an inviscid hyperbolic one-dimensional model and a viscous one was derived without the ansatz assumption and by section-averaging techniques. These models are

Inviscid model::

$$\left\{\begin{array}{rcl} \partial_t A + \partial_x Q & = & 0, \\ \partial_t Q + \partial_x(\frac{Q^2}{A} + \frac{1}{\rho}AP(A,x)) & = & \frac{1}{\rho}P(A,x)\partial_x A + 2\pi Rk\frac{Q}{A}, \end{array}\right. \tag{3}$$

Viscous model::

$$\left\{\begin{array}{rcl} \partial_t A + \partial_x Q & = & 0, \\ \partial_t Q + \partial_x(\frac{Q^2}{A} + \frac{1}{\rho}AP(A,x)) - \partial_x(3\nu A\partial_x(\frac{Q}{A})) & = & \frac{1}{\rho}P(A,x)\partial_x A + \frac{2\pi Rk}{1-\frac{Rk}{4\nu}}\frac{Q}{A}, \end{array}\right. \tag{4}$$

where $R(t,x)$ is the radius, $A = \pi R^2$ the area, $Q = A\overline{u_x}$ the flow rate, $\overline{u_x}$ the mean speed of blood per section, ρ the density of blood, P, the pressure, ν the kinematic viscosity, and k a negative friction coefficient. For these models, several mathematical and physical properties have been obtained (see [**?**] for further details).

These two new one-dimensional models, while similar to existing ones in the literature, are derived using a well-known technique used, for instance, in [9, 10, 14]. This method allows the construction of each asymptotic term one by one, distinguishing it from the classical approach using ansatz (see Eq. (1) and [19]). The most notable advantage of these one-dimensional models is the ease of implementation of fast and robust numerical methods and providing good results in the context of quasi-cylindrical arteries.

Although, in the presence of aneurysms, both previously derived models may suffer from precision issues due to the non-uniform deformation in the radial direction [15]. To avoid those issues a three-dimensional model can be used, however, it leads to costly numerical computations. This leads to our idea of developing the first two-dimensional blood flow model in complex artery geometry. This new model reads

$$
(5)\quad \begin{cases} \partial_t A + \partial_\theta(\frac{Q_{R\theta}}{A}) + \partial_s(Q_s) &= 0, \\ \partial_t(Q_{R\theta}) + \partial_\theta(\frac{Q_{R\theta}^2}{2A^2} + AP) + \partial_s(\frac{Q_{R\theta}Q_s}{A}) &= \frac{2R}{3}\mathcal{C}\sin\theta\frac{Q_s^2}{A} + 2Rk\frac{Q_{R\theta}}{A} + \partial_\theta AP, \\ \partial_t\left(Q_s\right) + \partial_\theta\left(\frac{Q_sQ_{R\theta}}{A^2}\right) + \partial_s\left(\frac{Q_s^2}{A} - \frac{Q_{R\theta}^2}{2A^2} + AP\right) &= -\frac{2R}{3}\mathcal{C}\sin\theta\frac{Q_sQ_{R\theta}}{A^2} + kR\frac{Q_s}{A} + \partial_s AP, \\ P &= P_{ext} + b\frac{R-R_0}{R_0^2}. \end{cases}
$$

where $A(t,\theta,s)$ is now define as $\frac{R^2}{2}$ with s the curvilinear abscissa and θ the angle, $Q_{R\theta} = \frac{3}{4}RA\overline{u_\theta}$, $Q_s = A\overline{u_s}$, P the pressure, $\mathcal{C}$ the curvature of the artery and k a negative friction coefficient. This new model takes into account the variations of the geometry more accurately than one-dimensional models and yields to less expensive numerical method than the three-dimensional ones.

We outline the rest of the paper as follows: in section 2, as our starting point we present the Navier-Stokes equations and the boundary conditions including friction and the wall law deformation. We derive the radial-averaged two-dimensional equations. In section 3, we use a Discontinues Galerkin (DG) method from [6] called the Runge-Kutta Discontinues Galerkin method (RKDG). We use explicit Runge-Kutta for time integration. We provide extensive numerical testing in section 4 of the resulting code. A Julia[1] implementation of this code, written by Y. Mannes and M. Ersoy, is freely available on request.

2. On the derivation of a new two-dimensional model for blood flow in arteries

In this section, we present the full derivation of the new two-dimensional model for blood flow (Eq. (5)) starting from the Navier-Stokes equations.

2.1. Navier-Stokes equations in a curvilinear coordinate system.

We aim to construct a mathematical model for blood flow in an artery consistent with the phenomena that can affect its motion. We propose a model reduction of the three-dimensional Navier-Stokes equations leading to a new two-dimensional model following the technique in [9, 10, 14]. We study the case of a curvilinear artery (with a star-like cross-section, see Figure 1) and consider suitable boundary conditions to account for artery wall radial deformation and friction. In contrast with existing models for which the radius is θ-independant, we assume here that the radius is a function of θ, thus yielding radial non-uniform deformation. This assumption allows us to, accurately, describe aneurysms, stenosis, etc.

Figure 1. Artery shape

[1] https://julialang.org/

We start in subsubsection 2.1.1 by reviewing the Navier-Stokes equations in a curvilinear coordinate frame (using a Serret-Frenet in a cylindrical framework), describing the physics with the artery wall boundary. We then introduce the boundary condition at the wall in subsubsection 2.1.2.

2.1.1. *Geometric set-up and the three-dimensional Navier-Stokes equations in curvilinear coordinates.* Regarding Figure 1, we consider arteries with star-like cross-sections, meaning, all cross-sections are convex to a curve $c \in C^3([0,L],\mathbb{R}^3)$ with L the length of the artery, and belong to the orthogonal plane to $c'(s)$, where s stands for the curvilinear abscissa. Moreover, we suppose c verifies $||c'(s)||_{\mathbb{R}^3} = 1$ for all $s \in [0,L]$ and $||c''(s)||_{\mathbb{R}^3} \neq 0$ for all $s \in [0,L]$.

We consider an incompressible fluid moving in the time-space domain

$$\Omega = \left\{(x,y,z) \in \mathbb{R}^3 \,;\, ||(x,y,z) - c(s(x,y,z))||_{\mathbb{R}^3} \leq R(t,x,y,z),\, s(x,y,z) \in [0,L],\, t \in [0,T]\right\}, \tag{6}$$

where, $s(x,y,z)$ is such that (x,y,z) belongs to the orthogonal plane of $c'(s)$ as displayed in Figure 2, $R(t,x,y,z)$ is the radius of the cross-section at a particular angle θ and $T > 0$ an arbitrary final time.

We assume that the velocity $\overrightarrow{u}$ of the viscous flow satisfies, on the domain Ω, the three-dimensional incompressible Navier-Stokes equations

$$\left\{ \begin{array}{rcl} div\, \overrightarrow{u} & = & 0, \\ \partial_t \overrightarrow{u} + div\,(\overrightarrow{u} \otimes \overrightarrow{u}) + \nabla p - div\, \sigma & = & 0, \end{array} \right. \tag{7}$$

where $\overrightarrow{u} = u_x \overrightarrow{i} + u_y \overrightarrow{j} + u_z \overrightarrow{k}$ with $(\overrightarrow{i}, \overrightarrow{j}, \overrightarrow{k})$ the cartesian basis, $p = \frac{P}{\rho}$ where P is the pressure and ρ, the density of the fluid. Finally, the stress tensor is $\sigma = \nu\left(\nabla \overrightarrow{u} + (\nabla \overrightarrow{u})^t\right)$ where ν is the kinematic viscosity. Consider the following change of variable,

$$\overrightarrow{e_r}(\theta,s) = \cos\theta\, \overrightarrow{n}(s) + \sin\theta\, \overrightarrow{b}(s), \qquad \overrightarrow{e_\theta}(\theta,s) = -\sin\theta\, \overrightarrow{n}(s) + \cos\theta\, \overrightarrow{b}(s), \tag{8}$$

where $\overrightarrow{t}(s) = c'(s)$, $\overrightarrow{n}(s) = \frac{c''(s)}{\mathcal{C}(s)}$, and $\overrightarrow{b}(s) = \overrightarrow{t}(s) \wedge \overrightarrow{n}(s)$ with $\mathcal{C}(s) = ||c''(s)||_{\mathbb{R}^3}$ for all $s \in [0,L]$, the curvature of the artery, then the domain Ω from Eq. (6) is expressed as

$$\Omega = \left\{c(s) + r\overrightarrow{e_r}(\theta,s) \in \mathbb{R}^3 \,|\, r \in [0,R(t,x)], \theta \in [0,2\pi[,\, s \in [0,L],\, t \in [0,T]\right\}\ .$$

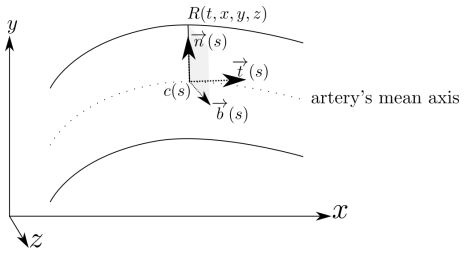

FIGURE 2. Serret Frenet Frame

The velocity $\overrightarrow{u} = u_r \overrightarrow{e_r} + u_\theta \overrightarrow{e_\theta} + u_s \overrightarrow{t}$ where u_r is the radial speed, u_θ is the angular speed and u_s is the axial speed.

The coordinate transformation reads $M(r,\theta,s) = c(s) + r\overrightarrow{e_r}(\theta,s)$ leading to the following Jacobian matrix, $A^{-1} = \begin{pmatrix} 1 & 0 & 0 \\ 0 & r & r\mathcal{T} \\ 0 & 0 & \beta \end{pmatrix}_{\overrightarrow{e_r},\overrightarrow{e_\theta},\overrightarrow{t}}$ where $\mathcal{T}(s) = \frac{1}{\mathcal{C}^2(s)} \det(c'(s), c''(s), c^{(3)}(s))$ is the torsion of the curve and $\beta(r,\theta,s) = 1 - r\mathcal{C}(s)\cos\theta$. The inverse Jacobian matrix then reads, $A =$

$\frac{1}{J}\begin{pmatrix} r\beta & 0 & 0 \\ 0 & \beta & -r\mathcal{T} \\ 0 & 0 & r \end{pmatrix}_{\overrightarrow{e_r},\overrightarrow{e_\theta},\overrightarrow{t}}$ where $J = r\beta = \det(A^{-1})$. Coordinate change in Eq. (8) leads to

$$\nabla p = \begin{pmatrix} \partial_r p \\ \frac{1}{r}\partial_\theta p \\ \frac{\partial_s p - \mathcal{T}(s)\partial_\theta p}{\beta} \end{pmatrix}_{\overrightarrow{e_r},\overrightarrow{e_\theta},\overrightarrow{t}} = \begin{pmatrix} \partial_r p \\ \frac{1}{r}\partial_\theta p \\ \frac{\partial_\mathcal{T} p}{\beta} \end{pmatrix}_{\overrightarrow{e_r},\overrightarrow{e_\theta},\overrightarrow{t}} \text{ where } \partial_\mathcal{T} = \partial_s - \mathcal{T}\partial_\theta, \text{ and,}$$

$$div\ \overrightarrow{u} = \frac{1}{r\beta}\partial_r(r\beta u_r) + \frac{1}{r\beta}\partial_\theta(\beta u_\theta) + \frac{1}{r\beta}\partial_\mathcal{T}(r u_s),$$

$$\nabla \overrightarrow{u} = \begin{pmatrix} \partial_r u_r & \partial_r u_\theta & \partial_r u_s \\ \frac{\partial_\theta u_r - u_\theta}{r} & \frac{\partial_\theta u_\theta + u_r}{r} & \frac{\partial_\theta u_s}{r} \\ \frac{\partial_\mathcal{T} u_r + \mathcal{C}\cos\theta u_s}{\beta} & \frac{\partial_\mathcal{T} u_\theta - \mathcal{C}\sin\theta u_s}{\beta} & \frac{\partial_\mathcal{T} u_s - \mathcal{C}(\cos\theta u_r - \sin\theta u_\theta)}{\beta} \end{pmatrix}_{\overrightarrow{e_r},\overrightarrow{e_\theta},\overrightarrow{t}},$$

$$div\,\sigma = \begin{pmatrix} \frac{1}{r\beta}\partial_r(r\beta\sigma_{rr}) + \frac{1}{r\beta}\partial_\theta(\beta\sigma_{\theta r}) + \frac{1}{r\beta}\partial_\mathcal{T}(r\sigma_{sr}) - \frac{1}{r}\sigma_{\theta\theta} + \frac{\mathcal{C}\cos\theta}{\beta}\sigma_{ss} \\ \frac{1}{r\beta}\partial_r(r\beta\sigma_{r\theta}) + \frac{1}{r\beta}\partial_\theta(\beta\sigma_{\theta\theta}) + \frac{1}{r\beta}\partial_\mathcal{T}(r\sigma_{s\theta}) + \frac{1}{r}\sigma_{\theta r} - \frac{\mathcal{C}\sin\theta}{\beta}\sigma_{ss} \\ \frac{1}{r\beta}\partial_r(r\beta\sigma_{rs}) + \frac{1}{r\beta}\partial_\theta(\beta\sigma_{\theta s}) + \frac{1}{r\beta}\partial_\mathcal{T}(r\sigma_{ss}) - \frac{\mathcal{C}}{\beta}(\cos\theta\sigma_{sr} - \sin\theta\sigma_{s\theta}) \end{pmatrix}_{\overrightarrow{e_r},\overrightarrow{e_\theta},\overrightarrow{t}},$$

where,

$$\sigma = \begin{pmatrix} \sigma_{rr} & \sigma_{r\theta} & \sigma_{rs} \\ \sigma_{\theta r} & \sigma_{\theta\theta} & \sigma_{\theta s} \\ \sigma_{sr} & \sigma_{s\theta} & \sigma_{ss} \end{pmatrix}_{\overrightarrow{e_r},\overrightarrow{e_\theta},\overrightarrow{t}} = \nu \begin{pmatrix} 2\partial_r u_r & \partial_r u_\theta + \frac{\partial_\theta u_r - u_\theta}{r} & \partial_r u_s + \frac{\partial_\mathcal{T} u_r + \mathcal{C}\cos\theta u_s}{\beta} \\ // & 2\frac{\partial_\theta u_\theta + u_r}{r} & \frac{\partial_\theta u_s}{r} + \frac{\partial_\mathcal{T} u_\theta - \mathcal{C}\sin\theta u_s}{\beta} \\ // & // & 2\frac{\partial_\mathcal{T} u_s - \mathcal{C}(\cos\theta u_r - \sin\theta u_\theta)}{\beta} \end{pmatrix}_{\overrightarrow{e_r},\overrightarrow{e_\theta},\overrightarrow{t}}. \tag{9}$$

Finally, the Navier Stokes equations from Eq. (7) in curvilinear coordinates from Eq. (8) are

Divergence equation:

$$\frac{1}{r\beta}\partial_r(r\beta u_r) + \frac{1}{r\beta}\partial_\theta(\beta u_\theta) + \frac{1}{r\beta}\partial_\mathcal{T}(r u_s) = 0, \tag{10}$$

Radial momentum equation:

$$\begin{aligned} &\partial_t u_r + \tfrac{1}{r\beta}\partial_r(r\beta u_r^2) + \tfrac{1}{r\beta}\partial_\theta(\beta u_r u_\theta) + \tfrac{1}{\beta}\partial_\mathcal{T}(u_r u_s) + \partial_r p - \tfrac{u_\theta^2}{r} + \tfrac{\mathcal{C}\cos\theta}{\beta}u_s^2 \\ &= \nu\left[\tfrac{2}{r\beta}\partial_r(r\beta\partial_r u_r) + \tfrac{1}{r\beta}\partial_\theta\left(\beta\left(\partial_r u_\theta + \tfrac{\partial_\theta u_r - u_\theta}{r}\right)\right) + \tfrac{1}{r\beta}\partial_\mathcal{T}\left(r\left(\partial_r u_s + \tfrac{\partial_\mathcal{T} u_r + \mathcal{C}\cos\theta u_s}{\beta}\right)\right)\right. \\ &\left. -\tfrac{2}{r}\tfrac{\partial_\theta u_\theta + u_r}{r} + \tfrac{\mathcal{C}\cos\theta}{\beta}\left(2\tfrac{\partial_\mathcal{T} u_s - \mathcal{C}(\cos\theta u_r - \sin\theta u_\theta)}{\beta}\right)\right] \end{aligned} \tag{11}$$

Angular momentum equation:

$$\begin{aligned} &\partial_t u_\theta + \tfrac{1}{r\beta}\partial_r(r\beta u_r u_\theta) + \tfrac{1}{r\beta}\partial_\theta(\beta u_\theta^2) + \tfrac{1}{\beta}\partial_\mathcal{T}(u_\theta u_s) + \tfrac{1}{r}\partial_\theta p + \tfrac{u_\theta u_r}{r} - \tfrac{\mathcal{C}\sin\theta}{\beta}u_s^2 \\ &= \nu\left[\tfrac{1}{r\beta}\partial_r\left(r\beta\left(\partial_r u_\theta + \tfrac{\partial_\theta u_r - u_\theta}{r}\right)\right) + \tfrac{2}{r\beta}\partial_\theta(\beta\tfrac{\partial_\theta u_\theta + u_r}{r}) + \tfrac{1}{r\beta}\partial_\mathcal{T}\left(r\left(\tfrac{\partial_\theta u_s}{r} + \tfrac{\partial_\mathcal{T} u_\theta - \mathcal{C}\sin\theta u_s}{\beta}\right)\right)\right. \\ &\left. +\tfrac{1}{r}\left(\partial_r u_\theta + \tfrac{\partial_\theta u_r - u_\theta}{r}\right) - \tfrac{\mathcal{C}\sin\theta}{\beta}\left(2\tfrac{\partial_\mathcal{T} u_s - \mathcal{C}(\cos\theta u_r - \sin\theta u_\theta)}{\beta}\right)\right] \end{aligned} \tag{12}$$

Axial momentum equation:

$$\begin{aligned} &\partial_t u_s + \tfrac{1}{r\beta}\partial_r(r\beta u_r u_s) + \tfrac{1}{r\beta}\partial_\theta(\beta u_\theta u_s) + \tfrac{1}{\beta}\partial_\mathcal{T}(u_s^2) + \tfrac{1}{\beta}\partial_\mathcal{T} p - \tfrac{\mathcal{C}}{\beta}(u_r\cos\theta - u_\theta\sin\theta)u_s \\ &= \nu\left[\tfrac{1}{r\beta}\partial_r\left(r\beta\left(\partial_r u_s + \tfrac{\partial_\mathcal{T} u_r + \mathcal{C}\cos\theta u_s}{\beta}\right)\right) + \tfrac{1}{r\beta}\partial_\theta\left(\beta\left(\tfrac{\partial_\theta u_s}{r} + \tfrac{\partial_\mathcal{T} u_\theta - \mathcal{C}\sin\theta u_s}{\beta}\right)\right)\right. \\ &+\tfrac{1}{r\beta}\partial_\mathcal{T}\left(r\left(2\tfrac{\partial_\mathcal{T} u_s - \mathcal{C}(\cos\theta u_r - \sin\theta u_\theta)}{\beta}\right)\right) \\ &\left. -\tfrac{\mathcal{C}}{\beta}\left(\cos\theta\left(\partial_r u_s + \tfrac{\partial_\mathcal{T} u_r + \mathcal{C}\cos\theta u_s}{\beta}\right) - \sin\theta\left(\tfrac{\partial_\theta u_s}{r} + \tfrac{\partial_\mathcal{T} u_\theta - \mathcal{C}\sin\theta u_s}{\beta}\right)\right)\right] \end{aligned} \tag{13}$$

2.1.2. *The artery wall boundary.* Crucial to our model derivation is the particular situation at the wall boundary, where the effect of wall deformation plays a central role. The wall boundary is the set of points

$$\Gamma = \{c(s) + R(t,\theta,s)\overrightarrow{e_r}(\theta,s) \mid \theta \in [0,2\pi[,\ s \in [0,L],\ t \in [0,T]\}\,.$$

We define Γ's tangential and outward normal vectors by

$$\overrightarrow{t_s^w} = \frac{1}{G_s}\left(\overrightarrow{t} + \frac{\partial_{\mathcal{T}} R}{\beta}\overrightarrow{e_r}\right), \quad \overrightarrow{t_\theta^w} = \frac{1}{G_\theta}\left(\overrightarrow{e_\theta} + \frac{\partial_\theta R}{R}\overrightarrow{e_r}\right), \quad \overrightarrow{n^w} = \frac{1}{G}\left(\overrightarrow{e_r} - \frac{\partial_\theta R}{R}\overrightarrow{e_\theta} - \frac{\partial_{\mathcal{T}} R}{\beta}\overrightarrow{t}\right),$$

where G_s, G_θ and G are the axial, circumferential and normal arclength

$$G_s = \sqrt{1 + \left(\tfrac{\partial_{\mathcal{T}} R}{\beta}\right)^2}, \quad G_\theta = \sqrt{1 + \left(\tfrac{\partial_\theta R}{R}\right)^2}, \quad G = \sqrt{1 + \left(\tfrac{\partial_\theta R}{R}\right)^2 + \left(\tfrac{\partial_{\mathcal{T}} R}{\beta}\right)^2}.$$

Since the wall is assumed to be rough, it produces friction, and due to its elastic behavior, it may get deformed. We take friction into account by considering the following Navier boundary condition on the wall Γ,

$$\left(\sigma\overrightarrow{n^w}\right)\cdot\overrightarrow{t_s^w} = k\,\overrightarrow{u}\cdot\overrightarrow{t_s^w}, \qquad \left(\sigma\overrightarrow{n^w}\right)\cdot\overrightarrow{t_\theta^w} = k\,\overrightarrow{u}\cdot\overrightarrow{t_\theta^w}, \tag{14}$$

where $k \leq 0$ is a friction term. Fluid-structure interaction is modeled with the condition

$$\overrightarrow{u}\cdot\overrightarrow{n^w} = \partial_t R\overrightarrow{e_r}\cdot\overrightarrow{n^w}. \tag{15}$$

As assumed in [19], thanks to the following hypothesis:

- **H1 :** Small thickness and plain stresses: the vessel wall thickness h is assumed to be, a constant, small enough to allow a shell-type representation of the artery geometry. The vessel structure is subjected to plain stresses.
- **H2 :** Radial displacement: the artery is described by a star-like cross-section around a curvilinear curve, and its displacements are only in the radial direction.
- **H3 :** Small deformation gradients and linear elastic behavior: we suppose that the artery wall behaves like a linear elastic solid where $\partial_{\mathcal{T}} R$ and $\partial_\theta R$ are assumed to be bounded in time.
- **H4 :** Incompressibility: the wall tissue is incompressible [13].
- **H5 :** Dominance of circumferential stresses. Stresses acting along the axial direction can be neglected compared to circumferential ones.

one can derive the wall dynamic law:

$$\partial_t^2\eta + \frac{\rho}{h\rho_w}b\frac{\eta}{R_0^2} = \frac{R}{R_0}\frac{\rho}{h\rho^w}\left[p - p_{\text{ext}} - G\sigma\overrightarrow{n^w}\cdot\overrightarrow{e_r}\right], \tag{16}$$

where $\eta = R - R_0$ is the displacement of the wall, $R_0 = R(t=0,\theta,s)$ is the initial radius of the artery, ρ^w is the wall tissues density, h is the wall thickness, p_{ext} is the external pressure $b(\theta,s) = \frac{E(\theta,s)h}{\rho(1-\xi^2)}$ is a function of the Young modulus E, σ from Eq. (9) is the fluid stress tensor at $r = R$, and p is the fluid pressure at $r = R$. Gathering Eqs. (14), (15) and (16), boundary conditions can be written:

Normal boundary condition

$$u_r - \frac{\partial_\theta R}{R}u_\theta - \frac{\partial_{\mathcal{T}} R}{\beta}u_s = \partial_t R, \tag{17}$$

Axial tangential boundary condition

$$\begin{aligned}&\nu\left[\partial_r u_s + \tfrac{\partial_{\mathcal{T}} u_r + \mathcal{C}\cos\theta u_s}{\beta} - \tfrac{\partial_\theta R}{R}\left(\tfrac{\partial_\theta u_s}{R} + \tfrac{\partial_{\mathcal{T}} u_\theta - \mathcal{C}\sin\theta u_s}{\beta}\right) - \tfrac{\partial_{\mathcal{T}} R}{\beta}\left(2\tfrac{\partial_{\mathcal{T}} u_s - \mathcal{C}(\cos\theta u_r - \sin\theta u_\theta)}{\beta}\right)\right.\\ &\left.+\tfrac{\partial_{\mathcal{T}} R}{\beta}\left(2\partial_r u_r - \tfrac{\partial_\theta R}{R}\left(\partial_r u_\theta + \tfrac{\partial_\theta u_r - u_\theta}{R}\right) - \tfrac{\partial_{\mathcal{T}} R}{\beta}\left(\partial_r u_s + \tfrac{\partial_{\mathcal{T}} u_r + \mathcal{C}\cos\theta u_s}{\beta}\right)\right)\right]\\ &= Gk(u_s + \tfrac{\partial_{\mathcal{T}} R}{\beta}u_r),\end{aligned} \tag{18}$$

Angular tangential boundary condition

$$
\begin{aligned}
&\nu\left[\partial_r u_\theta + \tfrac{\partial_\theta u_r - u_\theta}{R} - \tfrac{\partial_\theta R}{R}\left(2\tfrac{\partial_\theta u_\theta + u_r}{R}\right) - \tfrac{\partial_{\mathcal{T}} R}{\beta}\left(\tfrac{\partial_\theta u_s}{R} + \tfrac{\partial_{\mathcal{T}} u_\theta - \mathcal{C}\sin\theta u_s}{\beta}\right)\right.\\
&\left.+\tfrac{\partial_\theta R}{R}\left(2\partial_r u_r - \tfrac{\partial_\theta R}{R}\left(\partial_r u_\theta + \tfrac{\partial_\theta u_r - u_\theta}{R}\right) - \tfrac{\partial_{\mathcal{T}} R}{\beta}\left(\partial_r u_s + \tfrac{\partial_{\mathcal{T}} u_r + \mathcal{C}\cos\theta u_s}{\beta}\right)\right)\right]\\
&= Gk(u_\theta + \tfrac{\partial_\theta R}{R} u_r),
\end{aligned}
\tag{19}
$$

Wall dynamic law

$$
\begin{aligned}
&\tfrac{h\rho_w}{\rho}\tfrac{R_0}{R}\partial_t^2 R + b\tfrac{R-R_0}{RR_0}\\
&+\nu\left[2\partial_r u_r - \tfrac{\partial_\theta R}{R}\left(\partial_r u_\theta + \tfrac{\partial_\theta u_r - u_\theta}{R}\right) - \tfrac{\partial_{\mathcal{T}} R}{\beta}\left(\partial_r u_s + \tfrac{\partial_{\mathcal{T}} u_r + \mathcal{C}\cos\theta u_s}{\beta}\right)\right]\\
&= p - p_{ext}.
\end{aligned}
\tag{20}
$$

2.2. **Blood flow model with wall deformation via radial-averaging.** We now proceed to write the Navier-Stokes equations with boundary conditions in non-dimensional form. Next, under a thin-artery assumption, we consider the radius of the artery to be small compared to the length, introducing a small parameter ε. We formally make an asymptotic expansion of the Navier-Stokes system in first order with respect to ε. Finally, we derive a radial-averaged first-order two-dimensional model for blood flow. Our approach is similar to those used in [9, 19, 14, 10, 7].

2.2.1. *Dimensionless Navier-Stokes equations.* To derive the blood flow model, we assume that the artery's radius is small compared to its length and that radial variations in velocity are small compared to axial ones. This is achieved by postulating a small parameter ratio

$$\varepsilon := \frac{\overline{R}}{L} = \frac{U_r}{U_s} = \frac{U_r}{U_\theta} \ll 1,$$

where, $\overline{R}$, L, U_r, U_θ, and U_s are the scales of, respectively, radius, length, radial velocity, angular velocity, and axial velocity. As a consequence, the time scale T is such that $T = \frac{L}{U_s} = \frac{L}{U_\theta} = \frac{\overline{R}}{U_r}$. We also choose the pressure scale to be

$$\overline{p} = U_s^2 = U_\theta^2. \tag{21}$$

It is convenient to define L, U_s, U_θ and T, as finite constants with respect to ε, while $\overline{R} = \varepsilon L$ and $U_r = \varepsilon U_s = \varepsilon U_\theta$. This allows us to introduce the dimensionless quantities of time $\tilde{t}$, space ($\tilde{s}$,$\tilde{r}$,$\tilde{\theta}$), pressure $\tilde{p}$ and velocity field ($\tilde{u}_s$, $\tilde{u}_\theta$, $\tilde{u}_r$) via the following scaling relations

$$
\begin{aligned}
&\tilde{t} := \tfrac{t}{T}, && \tilde{p}(\tilde{t},\tilde{r},\tilde{\theta},\tilde{s}) = \tfrac{p(t,r,\theta,s)}{\overline{p}},\\
&\tilde{s} := \tfrac{s}{L}, && \tilde{u}_s(\tilde{t},\tilde{r},\tilde{\theta},\tilde{s}) = \tfrac{u_s(t,r,\theta,s)}{U_s},\\
&\tilde{r} := \tfrac{r}{\overline{R}} = \tfrac{r}{\varepsilon L}, && \tilde{u}_r(\tilde{t},\tilde{r},\tilde{\theta},\tilde{s}) = \tfrac{u_r(t,r,\theta,s)}{U_r},\\
&\tilde{\theta} := \tfrac{\theta}{\varepsilon}, && \tilde{u}_\theta(\tilde{t},\tilde{r},\tilde{\theta},\tilde{s}) = \tfrac{u_\theta(t,r,\theta,s)}{U_\theta}.
\end{aligned}
\tag{22}
$$

We also rescale the following coefficients

$$
\begin{aligned}
&\tilde{k} = \tfrac{k}{U_r} = \tfrac{k}{\varepsilon U_s} = \tfrac{k}{\varepsilon U_\theta}, && \tilde{R}(\tilde{t},\tilde{\theta},\tilde{s}) = \tfrac{R(t,\theta,s)}{\overline{R}},\\
&\tilde{h} = \tfrac{h}{\varepsilon\overline{R}}, && \tilde{E}(\tilde{\theta},\tilde{s}) = \varepsilon\tfrac{E(\theta,s)}{\rho U_s^2},\\
&\tilde{R}_0(\tilde{\theta},\tilde{s}) = \tfrac{R_0(\theta,s)}{\overline{R}} && \tilde{\mathcal{C}}(\tilde{s}) = L\mathcal{C}(s)\\
&\tilde{\mathcal{T}}(\tilde{s}) = L\mathcal{T}(s).
\end{aligned}
\tag{23}
$$

Finally, we define the non-dimensional Reynolds number $R_e = \frac{LU_s}{\nu}$ and $\nu_0 = (\varepsilon R_e)^{-1}$ yielding to the asymptotic regime

$$R_e^{-1} = \nu_0\varepsilon. \tag{24}$$

Let us also remark that

$$\beta(\tilde{r},\tilde{\theta},\tilde{s}) = 1-\varepsilon\tilde{r}\tilde{\mathcal{C}}\cos\theta = 1+O(\varepsilon) \text{ and } \partial_{\mathcal{T}} = \frac{1}{L}\partial_{\tilde{\mathcal{T}}} = \frac{1}{L}\left(\partial_{\tilde{s}} - \varepsilon\tilde{\mathcal{T}}\partial_{\tilde{\theta}}\right) = \frac{1}{L}\partial_{\tilde{s}} + O(\varepsilon).$$

With these assumptions, the effect of torsion is neglected.

Using these dimensionless variables Eqs. (21), (22), (23) and (24) in the Navier-Stokes equations from Eqs. (10), (11), (12), (13), we get

Dimensionless divergence equation:

$$\frac{1}{\tilde{r}\tilde{\beta}}\partial_{\tilde{r}}(\tilde{r}\tilde{\beta}\tilde{u}_r) + \frac{1}{\tilde{r}\tilde{\beta}}\partial_{\tilde{\theta}}(\tilde{\beta}\tilde{u}_\theta) + \frac{1}{\tilde{\beta}}\partial_{\tilde{\mathcal{T}}}(\tilde{u}_s) = 0, \tag{25}$$

Dimensionless radial momentum equation:

$$\partial_{\tilde{r}}\tilde{p} - \frac{\tilde{u}_\theta^2}{\tilde{r}} = \varepsilon\delta_{r\varepsilon}, \tag{26}$$

with

$$\begin{aligned}
\delta_{r\varepsilon} = \varepsilon&\left[\partial_{\tilde{t}}\tilde{u}_r + \frac{1}{\tilde{r}\tilde{\beta}}\partial_{\tilde{r}}(\tilde{r}\tilde{\beta}\tilde{u}_r^2) + \frac{1}{\tilde{r}\tilde{\beta}}\partial_{\tilde{\theta}}(\tilde{\beta}\tilde{u}_r\tilde{u}_\theta) + \frac{1}{\tilde{\beta}}\partial_{\tilde{\mathcal{T}}}(\tilde{u}_r\tilde{u}_s)\right] + \frac{\tilde{\mathcal{C}}\cos\tilde{\theta}}{\tilde{\beta}}\tilde{u}_s^2 \\
&-\nu_0\left[\frac{2}{\tilde{r}\tilde{\beta}}\partial_{\tilde{r}}(\tilde{r}\tilde{\beta}\partial_{\tilde{r}}\tilde{u}_r) + \frac{1}{\tilde{r}\tilde{\beta}}\partial_{\tilde{\theta}}\left(\tilde{\beta}\left(\partial_{\tilde{r}}\tilde{u}_\theta + \frac{\varepsilon^2\partial_{\tilde{\theta}}\tilde{u}_r - \tilde{u}_\theta}{\tilde{r}}\right)\right) - \frac{2}{\tilde{r}}\frac{\partial_{\tilde{\theta}}\tilde{u}_\theta + \tilde{u}_r}{\tilde{r}}\right. \\
&\left.+\frac{1}{\tilde{r}\tilde{\beta}}\partial_{\tilde{\mathcal{T}}}\left(\tilde{r}\left(\partial_{\tilde{r}}\tilde{u}_s + \frac{\varepsilon^2\partial_{\tilde{\mathcal{T}}}\tilde{u}_r + \varepsilon\tilde{\mathcal{C}}\cos\tilde{\theta}\tilde{u}_s}{\tilde{\beta}}\right)\right) + \varepsilon\frac{\tilde{\mathcal{C}}\cos\tilde{\theta}}{\tilde{\beta}}\left(2\frac{\partial_{\tilde{\mathcal{T}}}\tilde{u}_s - \tilde{\mathcal{C}}(\varepsilon\cos\tilde{\theta}\tilde{u}_r - \sin\tilde{\theta}\tilde{u}_\theta)}{\tilde{\beta}}\right)\right]
\end{aligned}$$

Dimensionless angular momentum equation:

$$\begin{aligned}
&\partial_{\tilde{t}}\tilde{u}_\theta + \tfrac{1}{\tilde{r}\tilde{\beta}}\partial_{\tilde{r}}(\tilde{r}\tilde{\beta}\tilde{u}_r\tilde{u}_\theta) + \tfrac{1}{\tilde{r}\tilde{\beta}}\partial_{\tilde{\theta}}(\tilde{\beta}\tilde{u}_\theta^2) + \tfrac{1}{\tilde{\beta}}\partial_{\tilde{\mathcal{T}}}(\tilde{u}_\theta\tilde{u}_s) + \tfrac{1}{\tilde{r}}\partial_{\tilde{\theta}}\tilde{p} + \tfrac{\tilde{u}_\theta\tilde{u}_r}{\tilde{r}} - \tfrac{\tilde{\mathcal{C}}\sin\tilde{\theta}}{\tilde{\beta}}\tilde{u}_s^2 \\
&= \tfrac{1}{\varepsilon}\nu_0\left[\tfrac{1}{\tilde{r}\tilde{\beta}}\partial_{\tilde{r}}\left(\tilde{r}\tilde{\beta}\left(\partial_{\tilde{r}}\tilde{u}_\theta - \tfrac{\tilde{u}_\theta}{\tilde{r}}\right)\right) + \tfrac{\partial_{\tilde{r}}\tilde{u}_\theta}{\tilde{r}} - \tfrac{\tilde{u}_\theta}{\tilde{r}^2}\right] + \varepsilon\delta_{\theta\varepsilon},
\end{aligned} \tag{27}$$

with

$$\begin{aligned}
\delta_{\theta\varepsilon} = \nu_0&\left[\frac{1}{\tilde{r}\tilde{\beta}}\partial_{\tilde{r}}\left(\tilde{r}\tilde{\beta}\left(\frac{\partial_{\tilde{\theta}}\tilde{u}_{\tilde{r}}}{\tilde{r}}\right)\right) + \frac{2}{\tilde{r}\tilde{\beta}}\partial_{\tilde{\theta}}(\tilde{\beta}\frac{\partial_{\tilde{\theta}}\tilde{u}_\theta + \tilde{u}_r}{\tilde{r}}) + \frac{1}{\tilde{r}\tilde{\beta}}\partial_{\tilde{\mathcal{T}}}\left(\tilde{r}\left(\frac{\partial_{\tilde{\theta}}\tilde{u}_s}{\tilde{r}} + \frac{\partial_{\tilde{\mathcal{T}}}\tilde{u}_\theta - \tilde{\mathcal{C}}\sin\tilde{\theta}\tilde{u}_s}{\tilde{\beta}}\right)\right)\right. \\
&\left.+\frac{1}{\tilde{r}}\left(\frac{\partial_{\tilde{\theta}}\tilde{u}_r}{\tilde{r}}\right) - \frac{\tilde{\mathcal{C}}\sin\tilde{\theta}}{\tilde{\beta}}\left(2\frac{\partial_{\tilde{\mathcal{T}}}\tilde{u}_s - \tilde{\mathcal{C}}(\varepsilon\cos\tilde{\theta}\tilde{u}_r - \sin\tilde{\theta}\tilde{u}_\theta)}{\tilde{\beta}}\right)\right]
\end{aligned}$$

Dimensionless axial momentum equation:

$$\begin{aligned}
&\partial_{\tilde{t}}\tilde{u}_s + \tfrac{1}{\tilde{r}\tilde{\beta}}\partial_{\tilde{r}}(\tilde{r}\tilde{\beta}\tilde{u}_r\tilde{u}_s) + \tfrac{1}{\tilde{r}\tilde{\beta}}\partial_{\tilde{\theta}}(\tilde{\beta}\tilde{u}_\theta\tilde{u}_s) + \tfrac{1}{\tilde{\beta}}\partial_{\tilde{\mathcal{T}}}(\tilde{u}_s^2) + \tfrac{1}{\tilde{\beta}}\partial_{\tilde{\mathcal{T}}}\tilde{p} + \tfrac{\tilde{\mathcal{C}}\sin\tilde{\theta}}{\tilde{\beta}}\tilde{u}_\theta\tilde{u}_s \\
&= \tfrac{\nu_0}{\varepsilon}\left[\tfrac{1}{\tilde{r}\tilde{\beta}}\partial_{\tilde{r}}\left(\tilde{r}\tilde{\beta}\partial_{\tilde{r}}\tilde{u}_s\right) - \varepsilon\tfrac{\tilde{\mathcal{C}}}{\tilde{r}\tilde{\beta}}\cos\tilde{\theta}\tilde{u}_s\right] + \varepsilon\delta_{s\varepsilon},
\end{aligned} \tag{28}$$

with

$$\begin{aligned}
\delta_{s\varepsilon} = \frac{\tilde{\mathcal{C}}\cos\tilde{\theta}}{\tilde{\beta}}\tilde{u}_r\tilde{u}_s + \nu_0&\left[\frac{1}{\tilde{r}\tilde{\beta}}\partial_{\tilde{r}}\left(\tilde{r}\partial_{\tilde{\mathcal{T}}}\tilde{u}_r\right) + \frac{1}{\tilde{r}\tilde{\beta}}\partial_{\tilde{\theta}}\left(\tilde{\beta}\left(\frac{\partial_{\tilde{\theta}}\tilde{u}_s}{\tilde{r}} + \frac{\partial_{\tilde{\mathcal{T}}}\tilde{u}_\theta - \tilde{\mathcal{C}}\sin\tilde{\theta}\tilde{u}_s}{\tilde{\beta}}\right)\right)\right. \\
&+\frac{1}{\tilde{r}\tilde{\beta}}\partial_{\tilde{\mathcal{T}}}\left(\tilde{r}\left(2\frac{\partial_{\tilde{\mathcal{T}}}\tilde{u}_s - \tilde{\mathcal{C}}(\varepsilon\cos\tilde{\theta}\tilde{u}_r - \sin\tilde{\theta}\tilde{u}_\theta)}{\tilde{\beta}}\right)\right) \\
&\left.-\frac{\tilde{\mathcal{C}}}{\tilde{\beta}}\left(\cos\tilde{\theta}\left(\frac{\varepsilon\partial_{\tilde{\mathcal{T}}}\tilde{u}_r + \tilde{\mathcal{C}}\cos\tilde{\theta}\tilde{u}_s}{\tilde{\beta}}\right) - \sin\tilde{\theta}\left(\frac{\partial_{\tilde{\theta}}\tilde{u}_s}{\tilde{r}} + \frac{\partial_{\tilde{\mathcal{T}}}\tilde{u}_\theta - \tilde{\mathcal{C}}\sin\tilde{\theta}\tilde{u}_s}{\tilde{\beta}}\right)\right)\right].
\end{aligned}$$

Similarly, the boundary conditions from Eqs. (17), (18), (19) and (20) become

Dimensionless normal boundary condition

$$\tilde{u}_r - \frac{\partial_{\tilde{\theta}}\tilde{R}}{\tilde{R}}\tilde{u}_\theta - \frac{\partial_{\tilde{\mathcal{T}}}\tilde{R}}{\beta}\tilde{u}_s = \partial_{\tilde{t}}\tilde{R}, \tag{29}$$

Dimensionless axial tangential boundary condition

$$\nu_0\partial_{\tilde{r}}\tilde{u}_s = \varepsilon\left(\tilde{G}\tilde{k}\tilde{u}_s - \nu_0\frac{\tilde{\mathcal{C}}\cos\tilde{\theta}}{\tilde{\beta}}\tilde{u}_s\right) + \varepsilon^2\delta_{Rs\varepsilon}, \tag{30}$$

with,

$$\delta_{Rs\varepsilon} = -\nu_0\left[\frac{\partial_{\tilde{\mathcal{T}}}\tilde{u}_r}{\tilde{\beta}} - \frac{\partial_{\tilde{\theta}}\tilde{R}}{\tilde{R}}\left(\frac{\partial_{\tilde{\theta}}\tilde{u}_s}{\tilde{R}} + \frac{\partial_{\tilde{\mathcal{T}}}\tilde{u}_\theta - \tilde{\mathcal{C}}\sin\tilde{\theta}\tilde{u}_s}{\tilde{\beta}}\right) - \frac{\partial_{\tilde{\mathcal{T}}}\tilde{R}}{\tilde{\beta}}\left(2\frac{\partial_{\tilde{\mathcal{T}}}\tilde{u}_s - \tilde{\mathcal{C}}(\varepsilon\cos\tilde{\theta}\tilde{u}_r - \sin\tilde{\theta}\tilde{u}_\theta)}{\tilde{\beta}}\right)\right.$$

$$\left.+\frac{\partial_{\tilde{\mathcal{T}}}\tilde{R}}{\tilde{\beta}}\left(2\partial_{\tilde{r}}\tilde{u}_r - \frac{\partial_{\tilde{\theta}}\tilde{R}}{\tilde{R}}\left(\varepsilon^2\partial_{\tilde{r}}\tilde{u}_\theta + \frac{\partial_{\tilde{\theta}}\tilde{u}_r - \tilde{u}_\theta}{\tilde{R}}\right) - \frac{\partial_{\tilde{\mathcal{T}}}\tilde{R}}{\tilde{\beta}}\left(\partial_{\tilde{r}}\tilde{u}_s + \frac{\varepsilon^2\partial_{\tilde{\mathcal{T}}}\tilde{u}_r + \varepsilon\tilde{\mathcal{C}}\cos\tilde{\theta}\tilde{u}_s}{\tilde{\beta}}\right)\right)\right]$$

$$+\tilde{G}\tilde{k}\frac{\partial_{\tilde{\mathcal{T}}}\tilde{R}}{\tilde{\beta}}\tilde{u}_r,$$

Dimensionless angular tangential boundary condition

$$\nu_0\left[\partial_{\tilde{r}}\tilde{u}_\theta - \frac{\tilde{u}_\theta}{\tilde{R}}\right] = \varepsilon\tilde{k}\tilde{u}_\theta + \varepsilon^2\delta_{R\theta\varepsilon}, \tag{31}$$

with

$$\delta_{R\theta\varepsilon} = -\nu_0\left[\frac{\partial_{\tilde{\theta}}\tilde{u}_r}{\tilde{R}} - \frac{\partial_{\tilde{\theta}}\tilde{R}}{\tilde{R}}\left(2\frac{\partial_{\tilde{\theta}}\tilde{u}_\theta + \tilde{u}_r}{\tilde{R}}\right) - \frac{\partial_{\tilde{\mathcal{T}}}\tilde{R}}{\tilde{\beta}}\left(\frac{\partial_{\tilde{\theta}}\tilde{u}_s}{\tilde{R}} + \frac{\partial_{\tilde{\mathcal{T}}}\tilde{u}_\theta - \tilde{\mathcal{C}}\sin\tilde{\theta}\tilde{u}_s}{\tilde{\beta}}\right)\right.$$

$$\left.+\frac{\partial_{\tilde{\theta}}\tilde{R}}{\tilde{R}}\left(2\partial_{\tilde{r}}\tilde{u}_r - \frac{\partial_{\tilde{\theta}}\tilde{R}}{\tilde{R}}\left(\partial_{\tilde{r}}\tilde{u}_\theta + \frac{\varepsilon^2\partial_{\tilde{\theta}}\tilde{u}_r - \tilde{u}_\theta}{\tilde{R}}\right) - \frac{\partial_{\tilde{\mathcal{T}}}\tilde{R}}{\tilde{\beta}}\left(\partial_{\tilde{r}}\tilde{u}_s + \frac{\varepsilon^2\partial_{\tilde{\mathcal{T}}}\tilde{u}_r + \varepsilon\tilde{\mathcal{C}}\cos\tilde{\theta}\tilde{u}_s}{\tilde{\beta}}\right)\right)\right]$$

$$+\tilde{G}\tilde{k}\frac{\partial_{\tilde{\theta}}\tilde{R}}{\tilde{R}}\tilde{u}_r,$$

Dimensionless wall dynamic law

$$\tilde{b}\frac{\tilde{R}-\tilde{R}_0}{\tilde{R}\tilde{R}_0} = \tilde{p} - \tilde{p}_{ext} + \varepsilon\delta_{R\varepsilon}, \tag{32}$$

with,

$$\delta_{R\varepsilon} = -\varepsilon^2\frac{\tilde{h}\rho_w}{\rho}\frac{\tilde{R}_0}{\tilde{R}}\partial_{\tilde{t}}^2\tilde{R}$$

$$-\nu_0\left[2\partial_{\tilde{r}}\tilde{u}_r - \frac{\partial_{\tilde{\theta}}\tilde{R}}{\tilde{R}}\left(\partial_{\tilde{r}}\tilde{u}_\theta + \frac{\varepsilon^2\partial_{\tilde{\theta}}\tilde{u}_r - \tilde{u}_\theta}{\tilde{R}}\right) - \frac{\partial_{\tilde{\mathcal{T}}}\tilde{R}}{\tilde{\beta}}\left(\partial_{\tilde{r}}\tilde{u}_s + \frac{\varepsilon^2\partial_{\tilde{\mathcal{T}}}\tilde{u}_r + \varepsilon\tilde{\mathcal{C}}\cos\tilde{\theta}\tilde{u}_s}{\tilde{\beta}}\right)\right]$$

where $\tilde{b}(\tilde{\theta},\tilde{s}) = \frac{\tilde{E}(\tilde{\theta},\tilde{s})h}{1-\xi^2}$.

2.2.2. *First order approximation of the dimensionless Navier-Stokes equations.* In the following, we omit the $\tilde{.}$. Identifying terms of order $\frac{1}{\varepsilon}$ in the axial momentum equation (28), we obtain the *motion by radius* (similar to the so-called *motion by slices*, see [14, 10, 8, 9]) decomposition

$$\nu_0 \frac{1}{r}\partial_r(r\partial_r u_s) = O(\varepsilon) \implies r\partial_r u_s = O(\varepsilon) \implies u_s(t,r,\theta,s) = u_{s,0}(t,\theta,s) + O(\varepsilon),$$

for some function $u_{s,0}$ and where we gathered all ε terms in $O(\varepsilon)$. Similarly, identifying terms of order $\frac{1}{\varepsilon}$ in the angular momentum equation (27), we obtain the motion by radial decomposition

$$\nu_0 \left[\frac{1}{r\beta}\partial_r\left(r\beta\left(\partial_r u_\theta - \frac{u_\theta}{r}\right)\right) + \frac{\partial_r u_\theta}{r} - \frac{u_\theta}{r^2}\right] = O(\varepsilon),$$

$$\implies \nu_0 \left[\frac{1}{r}\partial_r(r^2\partial_r\left(\frac{u_\theta}{r}\right)) + \partial_r\left(\frac{u_\theta}{r}\right)\right] = O(\varepsilon).$$

$$\implies \nu_0 \left[\partial_r\left(r\partial_r\left(\frac{u_\theta}{r}\right) + 2\frac{u_\theta}{r}\right)\right] = O(\varepsilon).$$

Using the angular tangential boundary condition from Eq. (31), it is straightforward to see that the only solution is,

$$\frac{u_\theta}{r} = \left(\frac{u_\theta}{r}\right)(r = R) + O(\varepsilon).$$

Noting

$$\overline{u_s}(t,\theta,s) = \frac{1}{A(t,\theta,s)}\int_0^{R(t,\theta,s)} r u_s(t,r,\theta,s)dr, \quad \overline{u_\theta}(t,\theta,s) = \frac{1}{A(t,\theta,s)}\int_0^{R} r u_\theta(t,r,\theta,s)dr,$$

as the mean axial and angular speeds of the fluid over a radius where

$$A(t,\theta,s) = \frac{R^2(t,\theta,s)}{2}, \tag{33}$$

we have the following properties:

$$u_s(t,r,\theta,s) = \overline{u_s}(t,\theta,s) + O(\varepsilon) \text{ and } \overline{u_s^2(t,r,\theta,s)} = \overline{u_s}^2(t,\theta,s) + O(\varepsilon), \tag{34}$$

$$u_\theta(t,r,\theta,s) = \frac{3}{2}\overline{u_\theta}(t,\theta,s)\frac{r}{R} + O(\varepsilon) \text{ and } \overline{u_\theta^2(t,r,\theta,s)} = \frac{9}{8}\overline{u_\theta}^2(t,\theta,s) + O(\varepsilon). \tag{35}$$

Multiplying by r and integrating the divergence equation (25) over a radius, we obtain

$$\begin{aligned} 0 &= \int_0^R [\partial_r(ru_r) + \partial_\theta(u_\theta) + \partial_s(ru_s)] + O(\varepsilon) \\ &= Ru_r(r=R) + \partial_\theta(\int_0^R u_\theta dr) - \partial_\theta R u_\theta(r=R) + \partial_s(\int_0^R r u_s dr) - \partial_s R R u_s(r=R) + O(\varepsilon). \end{aligned}$$

In view of the normal boundary condition from Eq. (29), we get the conservation equation

$$\partial_t A + \partial_\theta(\frac{3}{2}\frac{Q_\theta}{R}) + \partial_s(Q_s) = O(\varepsilon), \tag{36}$$

where,

$$Q_\theta(t,\theta,s) = A(t,\theta,s)\overline{u_\theta}(t,\theta,s) = \int_0^R r u_\theta dr, \quad Q_s(t,\theta,s) = A(t,\theta,s)\overline{u_s}(t,\theta,s) = \int_0^R r u_s dr. \tag{37}$$

Then, integrating the radial momentum equation (26) between r and R, we obtain the following pressure

$$p(t,r,\theta,s) = p(t,R,\theta,s) - \int_r^R \frac{u_\theta^2}{s}ds + O(\varepsilon) = p(t,R,\theta,s) - \frac{9}{8}\frac{Q_\theta^2}{A^2}\left(1 - \left(\frac{r}{R}\right)^2\right) + O(\varepsilon) \tag{38}$$

We proceed with multiplying by r^2 and integrating over a radius the angular momentum equation (27)

$$\begin{aligned}&\int_0^R r^2\left[\partial_t u_\theta+\tfrac{1}{r}\partial_r(ru_ru_\theta)+\tfrac{1}{r}\partial_\theta(u_\theta^2)+\partial_s(u_\theta u_s)+\tfrac{1}{r}\partial_\theta p+\tfrac{u_\theta u_r}{r}-\mathcal{C}\sin\theta u_s^2\right]dr\\&=\int_0^R r^2\left[\tfrac{1}{\varepsilon}\nu_0\left[\tfrac{1}{r}\partial_r\left(r\left(\partial_r u_\theta-\tfrac{u_\theta}{r}\right)\right)+\tfrac{\partial_r u_\theta}{r}-\tfrac{u_\theta}{r^2}\right]\right]dr+O(\varepsilon),\end{aligned}$$

yielding to

$$\begin{aligned}&\int_0^R r^2\partial_t u_\theta+\int_0^R\partial_r(r^2u_ru_\theta)+\int_0^R\partial_\theta(ru_\theta^2)+\int_0^R\partial_s(r^2u_\theta u_s)+\int_0^R\partial_\theta(rp)-\mathcal{C}\sin\theta\int_0^R r^2u_s^2\\&=\int_0^R\left[\tfrac{1}{\varepsilon}\nu_0\left[r\partial_r\left(r^2\partial_r\left(\tfrac{u_\theta}{r}\right)\right)+r^2\partial_r\left(\tfrac{u_\theta}{r}\right)\right]\right]+O(\varepsilon),\end{aligned}$$

and then,

$$\begin{aligned}&\int_0^R r^2\partial_t u_\theta+\int_0^R\partial_r(r^2u_ru_\theta)+\int_0^R\partial_\theta(ru_\theta^2)+\int_0^R\partial_s(r^2u_\theta u_s)+\int_0^R\partial_\theta(rp)-\mathcal{C}\sin\theta\int_0^R r^2u_s^2\\&=\int_0^R\partial_r\left[\tfrac{1}{\varepsilon}\nu_0\left[r^3\partial_r\left(\tfrac{u_\theta}{r}\right)\right]\right]+O(\varepsilon),\end{aligned}$$

Using the definitions of A in Eq. (33), Q_θ and Q_s in Eq. (37), thanks to the normal boundary condition from Eq. (29), we have

$$\begin{aligned}&\partial_t(\int_0^R r^2u_\theta)+\partial_\theta(\int_0^R ru_\theta^2)+\partial_s(\int_0^R r^2u_\theta u_s)+\partial_\theta\left(\int_0^R rp\right)-\partial_\theta Ap(r=R)-\mathcal{C}\sin\theta\int_0^R r^2u_s^2\\&=\tfrac{1}{\varepsilon}\nu_0\left[R^2\tfrac{\varepsilon}{\nu_0}ku_\theta(r=R)\right]+O(\varepsilon),\end{aligned}$$

Then, using the properties from Eq. (34) and Eq. (35), the expression of the pressure in Eq. (38) and the angular tangential boundary condition in Eq. (31), we obtain

(39)

$$\begin{aligned}&\partial_t(\tfrac{3R}{4}Q_\theta)+\partial_\theta(\tfrac{9R}{8}\tfrac{Q_\theta^2}{RA})+\partial_s(\tfrac{3R}{4}\tfrac{Q_\theta Q_s}{A})+\partial_\theta\left(Ap(r=R)-\tfrac{9R}{16}\tfrac{Q_\theta^2}{RA}\right)-\partial_\theta Ap(r=R)-\tfrac{2R}{3}\mathcal{C}\sin\theta\tfrac{Q_s^2}{A}\\&=\tfrac{3R}{2}Rk\tfrac{Q_\theta}{A}+O(\varepsilon),\end{aligned}$$

Finally, multiplying by r and integrating over a radius the axial momentum equation (28)

$$\begin{aligned}&\int_0^R r\left[\partial_t u_s+\tfrac{1}{r}\partial_r(ru_ru_s)+\tfrac{1}{r}\partial_\theta(u_\theta u_s)+\partial_s(u_s^2)+\partial_s p+\mathcal{C}\sin\theta u_\theta u_s\right]dr\\&=\int_0^R r\left[\tfrac{\nu_0}{\varepsilon}\left[\tfrac{1}{r\beta}\partial_r\left(r\beta\partial_r u_s\right)+\varepsilon\tfrac{\mathcal{C}\cos\theta}{r}u_s\right]\right]dr+O(\varepsilon),\end{aligned}$$

we get

$$\begin{aligned}&\int_0^R\partial_t\left(ru_s\right)+Ru_r(r=R)u_s(r=R)+\int_0^R\partial_\theta(u_\theta u_s)+\int_0^R\partial_s(ru_s^2)+\int_0^R\partial_s(rp)+\mathcal{C}\sin\theta\int_0^R ru_\theta u_s\\&=\int_0^R r\left[\tfrac{\nu_0}{\varepsilon}\left[\tfrac{1}{r\beta}\partial_r\left(r\beta\partial_r u_s\right)+\varepsilon\tfrac{\mathcal{C}\cos\theta}{r}u_s\right]\right]dr+O(\varepsilon),\end{aligned}$$

Using the definitions of A from Eq. (33), Q_θ and Q_s from Eq. (37), thanks to the normal boundary condition in Eq. (29), we have

$$\begin{aligned}&\partial_t\left(Q_s\right)+\partial_\theta\left(\int_0^R u_\theta u_s\right)+\partial_s\left(\int_0^R ru_s^2\right)+\partial_s\left(\int_0^R rp\right)-\partial_s Ap(r=R)+\mathcal{C}\sin\theta\int_0^R ru_\theta u_s\\&=\tfrac{\nu_0}{\varepsilon}\left[R(\partial_r u_s)(r=R)+\int_0^R\tfrac{\partial_r\beta}{\beta}r\partial_r u_s+\varepsilon\mathcal{C}\cos\theta\int_0^R u_s\right]+O(\varepsilon),\end{aligned}$$

Then, using the properties from Eq. (34) and Eq. (35), the expression of the pressure in Eq. (38) and the axial tangential boundary condition in Eq. (30), we obtain

$$\begin{aligned}&\partial_t\left(Q_s\right)+\partial_\theta\left(\tfrac{3}{2}\tfrac{Q_sQ_\theta}{AR}\right)+\partial_s\left(\tfrac{Q_s^2}{A}\right)+\partial_s\left(Ap(r=R)-\tfrac{9}{16}\tfrac{Q_\theta^2}{A}\right)-\partial_s Ap(r=R)\\&=kR\tfrac{Q_s}{A}-\mathcal{C}\sin\theta\tfrac{Q_sQ_\theta}{A}+O(\varepsilon),\end{aligned}$$

leading to

$$\begin{aligned}&\partial_t\left(Q_s\right)+\partial_\theta\left(\tfrac{3}{2}\tfrac{Q_sQ_\theta}{AR}\right)+\partial_s\left(\tfrac{Q_s^2}{A}-\tfrac{9}{16}\tfrac{Q_\theta^2}{A}+Ap(r=R)\right)\\&=kR\tfrac{Q_s}{A}-\mathcal{C}\sin\theta\tfrac{Q_sQ_\theta}{A}+\partial_s Ap(r=R)+O(\varepsilon).\end{aligned}\tag{40}$$

Finally from Eqs. (36), (39), (40) and the wall dynamic law in Eq. (32) dropping all terms of the first order, we obtain the following radial-averaged two-dimensional model for blood flow

$$\begin{cases} \partial_t A + \partial_\theta(\frac{3}{2}\frac{Q_\theta}{R}) + \partial_s(Q_s) &= 0, \\ \partial_t(\frac{3R}{4}Q_\theta) + \partial_\theta(\frac{9R}{16}\frac{Q_\theta^2}{RA} + Ap) + \partial_s(\frac{3R}{4}\frac{Q_\theta Q_s}{A}) &= \frac{2R}{3}\mathcal{C}\sin\theta\frac{Q_s^2}{A} + \frac{3R}{2}Rk\frac{Q_\theta}{A} + \partial_\theta Ap, \\ \partial_t\left(Q_s\right) + \partial_\theta\left(\frac{3}{2}\frac{Q_sQ_\theta}{AR}\right) + \partial_s\left(\frac{Q_s^2-\frac{9}{16}Q_\theta^2}{A} + Ap\right) &= kR\frac{Q_s}{A} - \mathcal{C}\sin\theta\frac{Q_sQ_\theta}{A} + \partial_s Ap, \\ p &= p_{ext} + b\frac{R-R_0}{R_0^2}. \end{cases}$$

where we have replaced $p(r = R = \sqrt{2A})$ by p for simplicity. Lastly, using a simple change of variable $Q_{R\theta} = \frac{3}{4}RQ_\theta$, we get,

$$\begin{cases} \partial_t A + \partial_\theta(\frac{Q_{R\theta}}{A}) + \partial_s(Q_s) &= 0, \\ \partial_t(Q_{R\theta}) + \partial_\theta(\frac{Q_{R\theta}^2}{2A^2} + Ap) + \partial_s(\frac{Q_{R\theta}Q_s}{A}) &= \frac{2R}{3}\mathcal{C}\sin\theta\frac{Q_s^2}{A} + 2Rk\frac{Q_{R\theta}}{A} + \partial_\theta Ap, \\ \partial_t\left(Q_s\right) + \partial_\theta\left(\frac{Q_sQ_{R\theta}}{A^2}\right) + \partial_s\left(\frac{Q_s^2}{A} - \frac{Q_{R\theta}^2}{2A^2} + Ap\right) &= -\frac{2R}{3}\mathcal{C}\sin\theta\frac{Q_sQ_{R\theta}}{A^2} + kR\frac{Q_s}{A} + \partial_s Ap, \\ p &= p_{ext} + b\frac{R-R_0}{R_0^2}. \end{cases} \tag{41}$$

2.2.3. *Mathematical properties for the two-dimensional model.* We have the following results

Theorem 1. *Let $(A, \overline{u_\theta}, \overline{u_s})$, and $Q_{R\theta} = \frac{3}{4}RQ_\theta = \frac{3}{4}RA\overline{u_\theta}$, $Q_s = A\overline{u_s}$ satisfy the two-dimensional blood flow system in Eq.* (41)*. Then, we have:*

(1) *System* (41) *is strictly hyperbolic if $A > 0$ and $Ap'(A) - \frac{9}{8}\overline{u_\theta}^2 \neq 0$.*

(2) *For smooth solution $(A, \overline{u_\theta}, \overline{u_s})$, in the region where $A > 0$, we have the following head equation,*

$$\partial_t\psi + \frac{3}{2}\frac{\overline{u_\theta}}{R}\partial_\theta(\psi + \overline{p}) + \overline{u_s}\partial_s(\psi + \overline{p}) + \frac{p - \overline{p}}{A}\partial_t A = \frac{9}{4A}Rk\overline{u_\theta}^2 + \frac{1}{A}kR\overline{u_s}^2. \tag{42}$$

where $\psi(u_\theta, u_s, p) = \frac{\frac{9}{8}u_\theta^2 + u_s^2}{2}$ is the total head and $\overline{p} = p - \frac{9}{16}\overline{u_\theta}^2$ is the mean pressure over a radius.

(3) *For smooth solution $(A, \overline{u_\theta}, \overline{u_s})$, the steady state reads $\overline{u_\theta} = 0$, $\overline{u_s} = 0$ and $p = p_0$ for some constant p_0. In particular, for $A = A_0$, we have $p_0 = 0$.*

(4) *The pair of function $(E, E + \tilde{p})$ with $E := A(\psi + p) - \tilde{p}$ forms a mathematical entropy pair for system* (41)*, in that they satisfy the following entropy relation for smooth solution $(A, \overline{u_\theta}, \overline{u_s})$:*

$$\partial_t E + \mathrm{d}iv_{\theta,s}\left(\begin{pmatrix}\frac{3}{2}\frac{\overline{u_\theta}}{R}\\ \overline{u_s}\end{pmatrix}\left(E + \tilde{p} - \frac{9}{16}A\overline{u_\theta}^2\right)\right) = \frac{9}{4}Rk\overline{u_\theta}^2 + kR\overline{u_s}^2.$$

(5) *The quantity E is consistent with the total energy energy $e = \frac{\varepsilon^2 u_r^2 + u_\theta^2 + u_s^2}{2}$ of the Navier-Stokes equations Eqs.* (25)– (28)*, in the sense that,*

$$\partial_t\left(\int_0^R re\right) + \int_0^R r\,\mathrm{d}iv\left(\overrightarrow{u}(e + p)\right) = \partial_t E + \mathrm{d}iv_{\theta,s}\left(\begin{pmatrix}\frac{3}{2}\frac{\overline{u_\theta}}{R}\\ \overline{u_s}\end{pmatrix}\left(E + \tilde{p} - \frac{9}{16}A\overline{u_\theta}^2\right)\right) + O(\varepsilon)$$

where $\overrightarrow{u} = \begin{pmatrix}\varepsilon u_r\\ u_\theta\\ u_s\end{pmatrix}$.

Remark 1. *The condition $Ap'(A) - \frac{9}{8}\overline{u_\theta}^2 \neq 0$ is always satisfied in real life situations* [13, 15].

Proof.

(1) To prove the hyperbolicity of system (41), we write

$$\partial_t U + H_\theta \partial_\theta U + H_s \partial_s U = S$$

where $U = \begin{pmatrix} A \\ Q_{R\theta} \\ Q_s \end{pmatrix}$, $H_\theta = \begin{pmatrix} -\frac{Q_{R\theta}}{A^2} & \frac{1}{A} & 0 \\ -\frac{Q_{R\theta}^2}{A^3} + Ap'(A) & \frac{Q_{R\theta}}{A^2} & 0 \\ -2\frac{Q_{R\theta}Q_s}{A^3} & \frac{Q_s}{A^2} & \frac{Q_{R\theta}}{A^2} \end{pmatrix}$,

$H_s = \begin{pmatrix} 0 & 0 & 1 \\ -\frac{Q_{R\theta}Q_s}{A^2} & \frac{Q_s}{A} & \frac{Q_{R\theta}}{A} \\ -\frac{Q_s^2}{A^2} + \frac{Q_{R\theta}^2}{A^3} + Ap'(A) & -\frac{Q_{R\theta}}{A^2} & 2\frac{Q_s}{A} \end{pmatrix}$, $S = \begin{pmatrix} 0 \\ \frac{2R}{3}\mathcal{C}\sin\theta\frac{Q_s^2}{A} + 2Rk\frac{Q_{R\theta}}{A} \\ -\frac{2R}{3}\mathcal{C}\sin\theta\frac{Q_sQ_{R\theta}}{A^2} + kR\frac{Q_s}{A} \end{pmatrix}$.

Then, remark that the eigenvalues for H_θ are $\mathrm{Sp}(H_\theta) = \left\{\frac{Q_{R\theta}}{A^2}, \sqrt{p'(A)}, -\sqrt{p'(A)}\right\}$. For H_s, the eigenvalues are $\mathrm{Sp}(H_s) = \left\{\frac{Q_s}{A}, \frac{Q_s}{A} - \sqrt{Ap'(A)}, \frac{Q_s}{A} + \sqrt{Ap'(A)}\right\}$. The system (41) is strictly hyperbolic if $A > 0$ and $\frac{Q_{R\theta}}{A^2} \neq \pm\sqrt{p'(A)}$ which can be written as $Ap'(A) - \frac{9}{8}\overline{u_\theta}^2 \neq 0$.

(2) Next, from simple manipulation, system (41) becomes,

$$\begin{cases} \partial_t A + \partial_\theta(\frac{3}{2}A\frac{\overline{u_\theta}}{R}) + \partial_s(A\overline{u_s}) &= 0, \\ \partial_t(\frac{3R}{4}A\overline{u_\theta}) + \partial_\theta(\frac{9R}{16}\frac{A\overline{u_\theta}^2}{R}) + \partial_s(\frac{3R}{4}A\overline{u_\theta u_s}) + A\partial_\theta p &= \frac{2R}{3}\mathcal{C}\sin\theta A\overline{u_s}^2 + \frac{3R}{2}Rk\overline{u_\theta}, \\ \partial_t\left(A\overline{u_s}\right) + \partial_\theta\left(\frac{3}{2}A\frac{\overline{u_s u_\theta}}{R}\right) + \partial_s\left(A\overline{u_s}^2 - \frac{9}{16}A\overline{u_\theta}^2\right) + A\partial_s p &= -\mathcal{C}\sin\theta A\overline{u_s u_\theta} + kR\overline{u_s}, \\ p &= p_{ext} + b\frac{R-R_0}{R_0^2}. \end{cases}$$

We first focus on the second equation, dividing by R, we have,

$$\partial_t(\tfrac{3}{4}A\overline{u_\theta}) + \partial_\theta(\tfrac{9}{16}\tfrac{A\overline{u_\theta}^2}{R}) + \partial_s(\tfrac{3}{4}A\overline{u_\theta u_s}) + \tfrac{3}{4R}A\overline{u_\theta}\left[\partial_t R + \tfrac{3}{4}\tfrac{\overline{u_\theta}}{R}\partial_\theta R + \overline{u_s}\partial_s R\right] + \tfrac{R}{2}\partial_\theta p = \tfrac{2}{3}\mathcal{C}\sin\theta A\overline{u_s}^2 + \tfrac{3}{2}Rk\overline{u_\theta}.$$

Then, we use the mass conservation equation (36) and divide by A to get,

$$\partial_t(\tfrac{3}{4}\overline{u_\theta}) + \tfrac{u_\theta}{R}\partial_\theta(\tfrac{9}{16}\overline{u_\theta}) - \tfrac{9}{16}\tfrac{\overline{u_\theta}}{A}\partial_\theta(A\tfrac{u_\theta}{R}) + \tfrac{3}{4R}\overline{u_\theta}\left[\partial_t R + \tfrac{3}{4}\tfrac{\overline{u_\theta}}{R}\partial_\theta R + \overline{u_s}\partial_s R\right] + u_s\partial_s(\tfrac{3}{4}\overline{u_\theta}) + \tfrac{R}{2A}\partial_\theta p = \tfrac{2}{3}\mathcal{C}\sin\theta\overline{u_s}^2 + \tfrac{3}{2A}Rk\overline{u_\theta}$$

which can be easily written as,

$$\partial_t(\frac{3}{4}\overline{u_\theta}) + \frac{3}{4R}\overline{u_\theta}\left[\partial_t R + \overline{u_s}\partial_s R\right] + u_s\partial_s(\frac{3}{4}\overline{u_\theta}) + \frac{1}{R}\partial_\theta p = \frac{2}{3}\mathcal{C}\sin\theta\overline{u_s}^2 + \frac{3}{2A}Rk\overline{u_\theta}.$$

Finally, we multiply by $\frac{3}{2}\overline{u_\theta}$ to get,

$$\partial_t(\frac{9}{16}\overline{u_\theta}^2) + \frac{9}{8R}\overline{u_\theta}^2\left[\partial_t R + \overline{u_s}\partial_s R\right] + u_s\partial_s(\frac{9}{16}\overline{u_\theta}^2) + \frac{3}{2}\frac{u_\theta}{R}\partial_\theta p = \mathcal{C}\sin\theta\overline{u_\theta u_s}^2 + \frac{9}{4A}Rk\overline{u_\theta}^2.$$

Similarly, for the third equation in system (41), using the divergence equation and dividing by A leads to,

$$\partial_t\left(\overline{u_s}\right) + \frac{3}{2}\frac{\overline{u_\theta}}{R}\partial_\theta\left(\overline{u_s}\right) + \overline{u_s}\partial_s\left(\overline{u_s}\right) - \frac{1}{A}\partial_s\left(\frac{9}{16}A\overline{u_\theta}^2\right) + \partial_s p = -\mathcal{C}\sin\theta\overline{u_s u_\theta} + \frac{1}{A}kR\overline{u_s},$$

and multiplying by $\overline{u_s}$,

$$\partial_t\left(\frac{\overline{u_s}^2}{2}\right) + \frac{3}{2}\frac{\overline{u_\theta}}{R}\partial_\theta\left(\frac{\overline{u_s}^2}{2}\right) + \overline{u_s}\partial_s\left(\frac{\overline{u_s}^2}{2}\right) - \frac{\overline{u_s}}{A}\partial_s\left(\frac{9}{16}A\overline{u_\theta}^2\right) + \overline{u_s}\partial_s p = -\mathcal{C}\sin\theta\overline{u_s}^2\overline{u_\theta} + \frac{1}{A}kR\overline{u_s}^2.$$

Finally gathering our two results we obtain,

$$\partial_t\psi + \tfrac{3}{2}\tfrac{\overline{u_\theta}}{R}\partial_\theta(\psi + p - \tfrac{9}{16}\overline{u_\theta}^2) + \overline{u_s}\partial_s(\psi + p) + \tfrac{9}{8R}\overline{u_\theta}^2\left[\partial_t R + \overline{u_s}\partial_s R\right] - \tfrac{\overline{u_s}}{A}\partial_s\left(\tfrac{9}{16}A\overline{u_\theta}^2\right) = \tfrac{9}{4A}Rk\overline{u_\theta}^2 + \tfrac{1}{A}kR\overline{u_s}^2$$

where $\psi = \frac{9}{16}\overline{u_\theta}^2 + \frac{1}{2}u_s^2$ is the total head. Reminding $\overline{p} = p - \frac{9}{16}\overline{u_\theta}^2$, we get,

$$\partial_t\psi + \frac{3}{2}\frac{\overline{u_\theta}}{R}\partial_\theta(\psi+\overline{p}) + \overline{u_s}\partial_s(\psi+\overline{p}) + \frac{p-\overline{p}}{A}\partial_t A = \frac{9}{4A}Rk\overline{u_\theta}^2 + \frac{1}{A}kR\overline{u_s}^2.$$

(3) The proof is based on simple algebraic computations and is left to the reader.

(4) We consider the head equation (42) and multiply by A,

$$\begin{aligned}&\partial_t(A\psi) - \psi\partial_t A + \partial_\theta(\tfrac{3}{2}\tfrac{A\overline{u_\theta}}{R}(\psi+\overline{p})) + \partial_s(A\overline{u_s}(\psi+\overline{p})) + (\psi+\overline{p})\partial_t A + (p-\overline{p})\partial_t A\\ &= \tfrac{9}{4}Rk\overline{u_\theta}^2 + kR\overline{u_s}^2,\end{aligned}$$

leading to

$$\partial_t(A(\psi+p)-\tilde{p}) + \partial_\theta(\frac{3}{2}\frac{A\overline{u_\theta}}{R}(\psi+\overline{p})) + \partial_s(A\overline{u_s}(\psi+\overline{p})) = \frac{9}{4}Rk\overline{u_\theta}^2 + kR\overline{u_s}^2,$$

with $\tilde{p}$ such that, $\tilde{p}'(A) = Ap'(A)$. We call energy the quantity $E := A(\psi+p) - \tilde{p}$ and remark,

$$\partial_t(E) + \partial_\theta\left(\frac{3}{2}\frac{\overline{u_\theta}}{R}(E+\tilde{p}-\frac{9}{16}A\overline{u_\theta}^2)\right) + \partial_s\left(\overline{u_s}(E+\tilde{p}-\frac{9}{16}A\overline{u_\theta}^2)\right) = \frac{9}{4}Rk\overline{u_\theta}^2 + kR\overline{u_s}^2.$$

Moreover, the total energy in our domain $\int_{-\pi}^{\pi}\int_0^L E ds d\theta$ decreases, *ie.*

$$\frac{d}{dt}(E_{tot}) = \frac{9}{4}(Rk)||\overline{u_\theta}||^2 + (Rk)||\overline{u_s}||^2 \leq 0,$$

with k supposed negative in the domain.

(5) In this proof, we use Eqs. (25), (26), (27), and (28) by omitting $\tilde{\cdot}$ and gathering all remainder terms in $O(\varepsilon)$. Multiplying respectively the radial momentum Eq. (26), angular momentum Eq. (27), and axial momentum Eq. (28) by u_r, u_θ, and u_s, and summing up the three equations obtained, one has

$$\begin{aligned}&\partial_t(\tfrac{u_\theta^2+u_s^2}{2}) + u_r\partial_r(\tfrac{u_\theta^2+u_s^2}{2}) + \tfrac{u_\theta}{r}\partial_\theta(\tfrac{u_\theta^2+u_s^2}{2}) + u_s\partial_s(\tfrac{u_\theta^2+u_s^2}{2}) + u_r\partial_r p + \tfrac{u_\theta}{r}\partial_\theta p + u_s\partial_s p\\ &= \tfrac{\nu_0}{\varepsilon}\left[\tfrac{u_s}{r\beta}\partial_r(r\beta\partial_r u_s) + \varepsilon\tfrac{\mathcal{C}\cos\theta}{r}u_s^2 + \tfrac{u_\theta}{r\beta}\partial_r\left(r\beta\left(\partial_r u_\theta - \tfrac{u_\theta}{r}\right)\right) + u_\theta\tfrac{\partial_r u_\theta}{r} - \tfrac{u_\theta^2}{r^2}\right] + O(\varepsilon).\end{aligned}$$

Defining $\phi = \frac{u_\theta^2+u_s^2}{2}$, recalling $e = \frac{\varepsilon^2u_r^2+u_\theta^2+u_s^2}{2}$,and therefore $e = \phi + O(\varepsilon^2)$, keeping it in mind, multiplying by $r\beta$ the previous equation, we have:

$$\begin{aligned}&\partial_t(r\phi) + \partial_r(ru_r(\phi+p)) + \partial_\theta(u_\theta(\phi+p)) + \partial_s(ru_s(\phi+p))\\ &= \tfrac{\nu_0}{\varepsilon}\left[u_s\partial_r(r\beta\partial_r u_s) + \varepsilon\mathcal{C}\cos\theta u_s^2 + \tfrac{u_\theta}{r}\partial_r\left(r^2\beta\left(\partial_r u_\theta - \tfrac{u_\theta}{r}\right)\right)\right] + O(\varepsilon).\end{aligned}$$

We proceed by integrating the above-equation, making use of the normal boundary condition from Eq. (29), to get:

$$\begin{aligned}&\partial_t(A\overline{\phi}) + \partial_\theta(\textstyle\int_0^R u_\theta(\phi+p)) + \partial_s(\int_0^R ru_s(\phi+p)) + \partial_t A p(r=R)\\ &= \tfrac{\nu_0}{\varepsilon}\textstyle\int_0^R\left[u_s\partial_r(r\beta\partial_r u_s) + \varepsilon\mathcal{C}\cos\theta u_s^2 + \tfrac{u_\theta}{r}\partial_r\left(r^2\beta\left(\partial_r u_\theta - \tfrac{u_\theta}{r}\right)\right)\right] + O(\varepsilon),\end{aligned}$$

where $\overline{\phi} = \frac{1}{A}\int_0^R r\phi$. Using the profile from Eqs. (35) and (34) we get,

$$\begin{aligned}&\partial_t(A(\overline{\phi}+p(r=R))-\tilde{p}) + \partial_\theta(\tfrac{3}{2}\tfrac{\overline{u_\theta}}{R}A(\overline{\phi}+\overline{p})) + \partial_s(\overline{u_s}A(\overline{\phi}+\overline{p}))\\ &= \tfrac{\nu_0}{\varepsilon}\left[\overline{u_s}R\beta(r=R)(\partial_r u_s)(r=R) + \varepsilon\mathcal{C}\cos\theta R\overline{u_s}^2\right.\\ &\left.+\tfrac{3}{2}\tfrac{\overline{u_\theta}}{R}\left(R^2\beta(r=R)\left((\partial_r u_\theta)(r=R) - \tfrac{u_\theta(r=R)}{R}\right)\right)\right] + O(\varepsilon),\end{aligned}$$

where $\tilde{p}$ is such that, $\tilde{p}'(A) = Ap'_R(A)$ with $p_R = p(r=R)$. Finally, using the boundary condition Eqs. (31) and (30) in the preceding equation, we get:

$$\begin{aligned}&\partial_t(A(\overline{\phi}+p(r=R))-\tilde{p}) + \partial_\theta(\tfrac{3}{2}\tfrac{\overline{u_\theta}}{R}A(\overline{\phi}+\overline{p})) + \partial_s(\overline{u_s}A(\overline{\phi}+\overline{p}))\\ &= \tfrac{\nu_0}{\varepsilon}\left[\overline{u_s}R(\tfrac{\varepsilon}{\nu_0}k\overline{u_s} - \varepsilon\mathcal{C}\cos\theta\overline{u_s}) + \varepsilon\mathcal{C}\cos\theta R\overline{u_s}^2 + \tfrac{9}{4}\overline{u_\theta}R\tfrac{\varepsilon}{\nu_0}k\overline{u_\theta}\right] + O(\varepsilon),\end{aligned}$$

yielding to

$$\begin{aligned}&\partial_t(A(\overline{\phi}+p(r=R))-\tilde{p})+\partial_\theta(\tfrac{3}{2}\tfrac{A\overline{u_\theta}}{R}(\overline{\phi}+\overline{p}))+\partial_s(A\overline{u_s}(\overline{\phi}+\overline{p}))\\&=Rk\overline{u_s}^2+\tfrac{9}{4}Rk\overline{u_\theta}^2+O(\varepsilon).\end{aligned}$$

Remarking that $\overline{\phi}=\frac{1}{A}\int_0^R r\frac{u_\theta^2+u_s^2}{2}dr=\psi$, we obtain the result:

$$\partial_t\left(\int_0^R re\right)+\int_0^R r\,\mathrm{d}iv\,(\overrightarrow{u}(e+p))=\partial_t E+\mathrm{d}iv_{\theta,s}\left(\begin{pmatrix}\frac{3}{2}\frac{\overline{u_\theta}}{R}\\ \overline{u_s}\end{pmatrix}\left(E+\tilde{p}-\frac{9}{16}A\overline{u_\theta}^2\right)\right)+O(\varepsilon).$$

□

3. A Discontinuous Galerkin method for the two-dimensional model

In this section, we present a discontinuous Galerkin method to solve a general two-dimensional hyperbolic system of equations, in particular for model (41), using the RKDG method from [6] on a cartesian grid. It can be easily generalized to non-conforming meshes (see for instance [**?**, **?**]).

3.1. **Model problem.** Our aim is to construct a high-order numerical method for the blood flow problem from Eq. (41) derived in section 2. To this purpose, we propose a Discontinuous Galerkin approach for two-dimensional hyperbolic problems following [6]. Let us consider the following non-linear two-dimensional hyperbolic problem:

$$\left\{\begin{array}{rcll}\partial_t u+\partial_x f_1+\partial_y f_2 &=& s, & \forall(t,x,y)\in]0,T]\times]a_1,b_1[\times]a_2,b_2[,\\ u(t=0,x,y) &=& u_0(x,y), & \forall(x,y)\in[a_1,b_1]\times[a_2,b_2],\\ u(t,x=a_1,y) &=& u_{\text{left}}(t,y), & \forall(t,y)\in]0,T]\times[a_2,b_2[,\\ u(t,x=b_1,y) &=& u_{\text{right}}(t,y), & \forall(t,y)\in]0,T]\times[a_2,b_2[,\\ u(t,x,y=a_2) &=& u_{\text{bottom}}(t,x), & \forall(t,x)\in]0,T]\times[a_1,b_1[,\\ u(t,x,y=b_2) &=& u_{\text{top}}(t,x), & \forall(t,x)\in]0,T]\times[a_1,b_1[.\end{array}\right. \tag{43}$$

where $(u_{\text{right}},u_{\text{left}},u_{\text{top}},u_{\text{bottom}})\in(\mathbb{R}^d)^4$ are Dirichlet boundary conditions and $u_0(x,y)\in\mathbb{R}^d$ is the initial condition. Here $f_1(t,x,y,u)\in\mathbb{R}^d$ is the advection component in the x direction, $f_2(t,x,y,u)$ is the advection component in the y direction, and $s(t,x,y,u,\nabla_{x,y}u)$ is the source term.

3.2. **Space discretization.** Since the objective is to solve Eq. (43) using a numerical scheme, defining a partition of the computational domain $[a_1,b_1]\times[a_2,b_2]$ is mandatory. For simplicity, a cartesian fixed mesh is used and its description is given in subsubsection 3.2.1. Following this description, we derive the discrete variational formulation in subsubsection 3.2.2. Finally, this will lead to an ODE system in subsubsection 3.2.3.

3.2.1. *Mesh description.* Let us define $\mathcal{E}$ a partition of the computational domain $[a_1,b_1]\times[a_2,b_2]$. The set of all open faces of all elements $E\in\mathcal{E}$ is denoted by $\mathcal{F}$. Moreover, we can define two subsets of $\mathcal{F}$, $\mathcal{F}^\partial$ for the boundary faces and $\mathcal{F}^{\text{in}}$ for the interior faces.

For a given element $E\in\mathcal{E}$, there exists a set of face $\mathcal{F}^E=\{F\in\mathcal{F}\,|\,F\in\partial E\}$ which defines boundaries of E. Then, for all interior faces of E, *i.e.* $\forall F\in\mathcal{F}^E\cap\mathcal{F}^{\text{in}}$, there exists a neighboring element E_r such that $E\cap E_r=F$. Consequently, the normal unit vector $\overrightarrow{n}_{E,F}:=\begin{pmatrix}n_x\\ n_y\end{pmatrix}$ pointing from E to E_r is well defined. Moreover for all boundary faces of E, *i.e.*, $\forall F\in\mathcal{F}^E\cap\mathcal{F}^\partial$, there exists E_∂ a fictitious element such that $E\cap E_\partial=F$. Again, $\overrightarrow{n}_{E,F}$ is well defined.

For simplicity, all elements are considered rectangular and faces are straight lines with normal vector $\overrightarrow{n}_{E,F}=\begin{pmatrix}\pm1\\ 0\end{pmatrix}$ for vertical faces or $\overrightarrow{n}_{E,F}=\begin{pmatrix}0\\ \pm1\end{pmatrix}$ for horizontal ones.

In the discontinuous Galerkin framework, the solutions are considered piecewise polynomials per element. Many basis exist for the polynomial space over an element as monomial, Legendre,

Dubiner, and others [5, **?**]. For simplicity, we only consider the monomial basis in this section. Finally, the approximate space is given as

$$V_p(\mathcal{E}) = \left\{ v : [a_1, b_1] \times [a_2, b_2] \to \mathbb{R} \,;\, v_{|_E} \in \mathbb{P}^p(E),\, \forall E \in \mathcal{E} \right\}.$$

3.2.2. *Weak formulation.* By multiplying the system (43) by a test function $v \in V_p(\mathcal{E})$ and integrating over an element E, we obtain

$$\int_E \partial_t uv - \int_E (f_1 \partial_x v + f_2 \partial_y v) dE + \sum_{F \in \mathcal{F}^E} \int_F \begin{pmatrix} f_1 \\ f_2 \end{pmatrix} \cdot \overrightarrow{n}_{E,F} v_{|_E} dF = \int_E svdE.$$

We look for $u_{DG} \in V_p(\mathcal{E})$ such that

$$\int_E \partial_t u_{DG} v - \int_E (f_1 \partial_x v + f_2 \partial_y v) dE + \sum_{F \in \mathcal{F}^E} \int_F \hat{f} v_{|_E} dF = \int_E svdE. \tag{44}$$

where $\hat{f}$ is the numerical flux which we choose, for simplicity, as the Rusanov flux

$$\hat{f}(t, x, y, u_{DG}, \overrightarrow{n}_{E,F}) = \left\{ \begin{pmatrix} f_1(t, x, y, u_{DG}) \\ f_2(t, x, y, u_{DG}) \end{pmatrix} \cdot \overrightarrow{n}_{E,F} \right\} + \frac{c}{2}[u_{DG}],$$

where $c = \max_{i=1,\dots,d} |\lambda_i(t, x_n, u, \overrightarrow{n})|$ with λ_i the eigenvalues of $\begin{pmatrix} \nabla_u f_1 \\ \nabla_u f_2 \end{pmatrix} \cdot \overrightarrow{n}$, $\{v\} = \frac{v_{|_E} + v_{|_{E_r}}}{2}$ the average of v at the face F and $[v] = v_{|_E} - v_{|_{E_r}}$ the jump of v across the face F. Remark that, for a face $F \in F^\partial$, we consider $u_{DG}|_{E^\partial}(F) = u_{\text{boundary}}$ where u_{boundary} are the boundary conditions set in Eq. (43).

3.2.3. *ODE system.* Consider the monomial two-dimensional basis functions of $\mathbb{P}_p(E)$ defined as $nbc = \frac{(p+1)(p+2)}{2}$ function defined by,

$$\varphi_i^E(x, y) = \varphi^E_{\frac{k(k+1)}{2}+j}(\hat{x}, \hat{y}) = \hat{x}^{k-j} \hat{y}^j, \tag{45}$$

where $0 \le k \le p$, $0 \le j \le k$ and, $\hat{x} = \frac{2}{h_x}(x - x_{n+\frac{1}{2}})$, $\quad \hat{y} = \frac{2}{h_y}(y - y_{n+\frac{1}{2}})$, with h_x and h_y the length and the width of the element E respectively. We look for a solution u_{DG} of Eq. (44) in $V_p(\mathcal{E})$ that we decompose in the basis Eq. (45):

$$u_{DG}(t, x, y) = \sum_{E \in \mathcal{E}} \sum_{i=0}^{nbc} \varphi_i^E(x, y) U_i^E(t) \mathbb{1}_E(x, y),$$

where the coefficients $U_i^E(t)$ are unknown time-dependent functions and $\mathbb{1}(x, y)$ is the characteristic function of the element E. Similarly, $v(x, y) = \sum_{E \in \mathcal{E}} \sum_{i=0}^{nbc} \varphi_i^E(x, y) V_i^E \mathbb{1}_E(x, y)$, with V_i^E constant coefficients. Following these definitions, one can write:

$$\begin{aligned} &\textstyle\sum_{E \in \mathcal{E}} \sum_{i=0}^{nbc} \sum_{j=0}^{nbc} \left(\int_E \phi_i^E \phi_j^E \right) \partial_t U_i^E V_j^E - \sum_{E \in \mathcal{E}} \sum_{j=0}^{nbc} \int_E (f_1 \partial_x \phi_j^E + f_2 \partial_y \phi_j^E) dE V_j^E \\ &+ \textstyle\sum_{E \in \mathcal{E}} \sum_{j=0}^{nbc} \sum_{F \in \mathcal{F}^E} \int_F \hat{f} \phi_j^E dF V_j^E = \sum_{E \in \mathcal{E}} \sum_{j=0}^{nbc} \int_E s \phi_j^E dE V_j^E. \end{aligned}$$

Finally, this can be written in matrix form as,

$$V^t M \partial_t U - V^t F(t, U) = V^t S(t, U),$$

where, $U = (U_i^E)_{i \in [\![1,nbc]\!], E \in \mathcal{E}}$, $\quad V = (V_i^E)_{i \in [\![1,nbc]\!], E \in \mathcal{E}}$, $\quad M = \left(\int_E \phi_i^E \phi_j^E \right)_{i \in [\![1,nbc]\!], j \in [\![1,nbc]\!], E \in \mathcal{E}}$, $F(t, U) = \left(\int_E (f_1 \partial_x \phi_j^E + f_2 \partial_y \phi_j^E) dE - \sum_{F \in \mathcal{F}^E} \int_F \hat{f} \phi_j^E dF \right)_{j \in [\![1,nbc]\!], E \in \mathcal{E}}$ and

$S(t,U) = \left(\int_E s\phi_j^E dE\right)_{j\in[\![1,nbc]\!],E\in\mathcal{E}}$. Simplifying by V^t, we get the following ODE system

$$M\partial_t U = F(t,U) + S(t,U). \tag{46}$$

3.3. **Time discretization.** In this section, we propose a time discretization based on the Runge–Kutta (RK) methods applied to the ODE system (46).

3.3.1. *RK methods.* We recall the RK methods presented in [**?**]. RK methods are used to solve a system of ODEs of the form

$$U'(t) = R(t,U) \tag{47}$$

where R is some function. Let $t_k \in [0,T]$ and Δt a well-chosen time step, s-stage-Runge-Kutta methods reads, for $i \in [\![1,s]\!]$,

$$\begin{cases} K^{(i)} = U^{(k)} + \Delta t \sum_{j=1}^s a_{ij} R(t_k + c_j\Delta t, K^{(j)}), \\ U^{(k+1)} = U^{(k)} + \Delta t \sum_{i=1}^s b_i R(t_k + c_i\Delta t, K^{(i)}), \end{cases}$$

where $U^{(k)} \approx U(t_k)$ is the approximate solution of Eq. (47) at time t_k and $U^{(k+1)} \approx U(t_k+\Delta t)$ the approximate solution at time $t_{k+1} = t_k + \Delta t$. The Butcher coefficient $(a_{ij})_{i\in[\![1,s]\!],j\in[\![1,s]\!]}$, $(b_i)_{i\in[\![1,s]\!]}$, $(c_i)_{i\in[\![1,s]\!]}$ are constrained, at a minimum, by certain order of accuracy and stability considerations as discussed in [**?**].

3.3.2. *Application to the ODE system.* We write the ODE from Eq. (46) in the form of Eq. (47) leading to, $\partial_t(U) = M^{-1}R(t,U)$ with $R(t,U) = F(t,U) + S(t,U)$ leading to the following scheme

$$\begin{cases} MK^{(i)} = MU^{(k)} + \Delta t \sum_{j=1}^s a_{ij} R(t_k + c_j\Delta t, K^{(j)}), \\ MU^{(k+1)} = MU^{(k)} + \Delta t \sum_{i=1}^s b_i R(t_k + c_i\Delta t, K^{(i)}), \end{cases} \tag{48}$$

The time step is given by

$$\Delta t = \frac{\text{cfl}}{2p+1} \min_{E\in\mathcal{E}} \frac{\text{Area}(E)}{\text{Diam}(E)} \frac{1}{c^k},$$

where cfl $\in]0,1]$, p is the polynomial degree, Area(E), the area of an element, Diam(E) its diameter and c^k, the characteristic speed define as $c^k = \max_{E\in\mathcal{E}} |\lambda(t_k, U^k, E)|$, with $\lambda(t,u,E)$ the maximum of the eigenvalues of $\nabla_u f_1(t,x,y,u) + \nabla_u f_2(t,x,y,u)$ for $(x,y) \in E$. This CFL condition is obtained by a von Neumann stability analysis of the RKDG methods [**?**, **?**].

We use the following explicit time scheme depending on p (see Table 1) and butcher tables can be found in [**?**, **?**]. Those algorithms are sometimes called TVD - RK (Total Variation Diminishing - RK) scheme or SSP-RK (Strong Stability Preserving - RK) scheme.

TABLE 1. Time schemes for different values of p

p	Time scheme
0	Euler
1	TVDRK2
2	TVDRK3
3	TVDRK4
4	TVDRK5

3.4. **Still-steady states solutions.** One can easily obtain a well-balanced scheme for the two-dimensional blood flow problem in Eq. (41) derived in section 2 by a simple change of variable. This is an important stability property of the numerical scheme. It is achieved by introducing the change of variable

$$a = A - A_0.$$

Thus, one can write the system (41) as

(49)
$$\begin{cases} \partial_t(a) + \partial_\theta(\frac{Q_{R\theta}}{a+A_0}) + \partial_s(Q_s) &= 0, \\ \partial_t(Q_{R\theta}) + \partial_\theta(\frac{Q_{R\theta}^2}{2(a+A_0)^2} + (a+A_0)p) + \partial_s(\frac{Q_{R\theta}Q_s}{a+A_0}) &= \frac{2R}{3}\mathcal{C}\sin\theta\frac{Q_s^2}{a+A_0} \\ & \quad +2Rk\frac{Q_{R\theta}}{a+A_0} + \partial_\theta(a+A_0)p, \\ \partial_t(Q_s) + \partial_\theta\left(\frac{Q_sQ_{R\theta}}{(a+A_0)^2}\right) + \partial_s\left(\frac{Q_s^2}{a+A_0} - \frac{Q_{R\theta}^2}{2(a+A_0)^2} + (a+A_0)p\right) &= -\frac{2R}{3}\mathcal{C}\sin\theta\frac{Q_sQ_{R\theta}}{(a+A_0)^2} \\ & \quad +kR\frac{Q_s}{(a+A_0)} + \partial_s(a+A_0)p, \\ p &= p_{ext} + b\frac{R-R_0}{R_0^2}. \end{cases}$$

Then, we have the following property :

Proposition 1. *The numerical scheme in Eq.* (48) *preserves exactly the still-steady states solutions (see Theorem 1).*

The proof is based on the recursivity principle and is left to the reader.

4. Test cases

In this chapter, we present several test cases for the Discontinuous Galerkin (DG) method developed in section 3 for the two-dimensional blood flow system (41). The main objective of these test cases is to evaluate the robustness of the DG method. From now on, we consider the model (49) instead of Eq. (41).

4.1. **Convergence order.** To solve the two-dimensional blood flow model (see section 2), we use the DG method presented in section 3. We aim to compute the numerical order of convergence for a given exact solution. We consider the following friction coefficient $k = -11\frac{\nu}{R}$. We also recall the pressure $p = b\frac{\sqrt{A}-\sqrt{A_0}}{A_0}$ with β a physical parameter for the wall. The physical and numerical parameters used are given in Table 2 together with the following geometric parameters: $\overrightarrow{c}(s) = \frac{(\cos(s),\sin(s),s)}{\sqrt{2}}$, leading to, $\overrightarrow{t}(s) = \frac{(-\sin(s),\cos(s),1)}{\sqrt{2}}$, and, $\overrightarrow{n}(s) = (-\cos(s),-\sin(s),0)$ where $\mathcal{C}(s) = \sqrt{2}$. We compute a reference solution for the $2D$ numerical scheme, as shown in Figure 3 using 128×128 elements. In Figure 4, we compute the convergence order for $N \times N$ elements with $N = 4$, 8, 16. We compute the error $\epsilon = ||u_{REF} - u_{DG}||_{l^2([0,1])}$ with u_{REF} the reference solution calculated before and u_{DG} the solution obtain at time $t = T$. We show that all variables converge at an order of $p+1$ in agreement with the classical result in the literature on the RKDG schemes (see for instance [6]).

4.2. **Stationary solutions.** For this test case, the aim is to show that the numerical method captures exactly the still-steady state solutions. We have used the following parameters in Table 3 and the following geometrical parameters: $\overrightarrow{c}(s) = (s, e^{-\frac{1}{2}(s-\frac{L}{2})^2}, 0)$, leading to, $\overrightarrow{t}(s) = \frac{(1,-(s-\frac{L}{2})e^{-\frac{1}{2}(s-\frac{L}{2})^2},0)}{\sqrt{1+(s-\frac{L}{2})^2e^{-(s-\frac{L}{2})^2}}}$, and, $\overrightarrow{n}(s) = \frac{(0,((s-\frac{L}{2})^2-1)e^{-\frac{1}{2}(s-\frac{L}{2})^2},0)}{|(s-\frac{L}{2})^2-1|e^{-\frac{1}{2}(s-\frac{L}{2})^2}} = (0, sign\left((s-\frac{L}{2})^2-1\right), 0)$,

where $\mathcal{C}(s) = \frac{||c''(s)||}{||c'(s)||} = \frac{|(s-\frac{L}{2})^2-1|e^{-\frac{1}{2}(s-\frac{L}{2})^2}}{\sqrt{1+(s-\frac{L}{2})^2e^{-(s-\frac{L}{2})^2}}}$. The initial geometry is represented in Figure 5 and

TABLE 2. Parameters for the convergence test

Parameter	Value
β	3
A_0	2
ν	3×10^{-2}
T	1
L	10
cfl	0.5

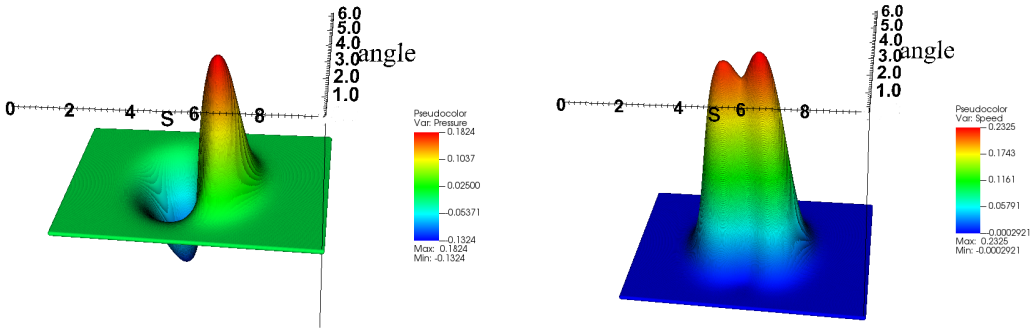

(A) Pressure (B) Speed

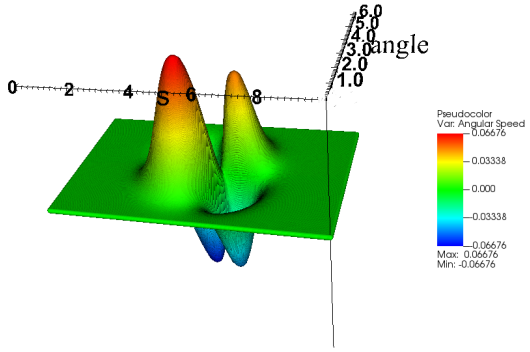

(C) Angular Speed

FIGURE 3. Reference solution for the $2D$ numerical scheme

it is defined by $A_0(x,\theta) = \frac{1}{2}\left(R_0 + (R_1 - R_0)e^{-4(x-\frac{L}{2})-2(\theta-\pi)}\right)^2$. and characterized by $\beta(x,\theta) = \left(E_0 + (E_1 - E_0)e^{-4(x-\frac{L}{2})-2(\theta-\pi)}\right)\frac{h\sqrt{2}}{2\rho(1-\xi^2)}$. Starting with a null speed, $A = A_0$, as in proved in Theorem 1, in Figure 6, we show that the still-steady state's solutions are exactly preserved.

4.3. **Realistic pressure wave in a straight artery.** In this test case, we compare the one-dimensional models $1D$ inviscid from Eq. (3) (solved by a DG method, see [**?**], and TGS-Taylor Galerkin Scheme, see [19]), $1D$ viscous from Eq. (4) (solved by a DG method, see [**?**]), and $2D$ Eq. (41) solved by the DG method presented in section 3.

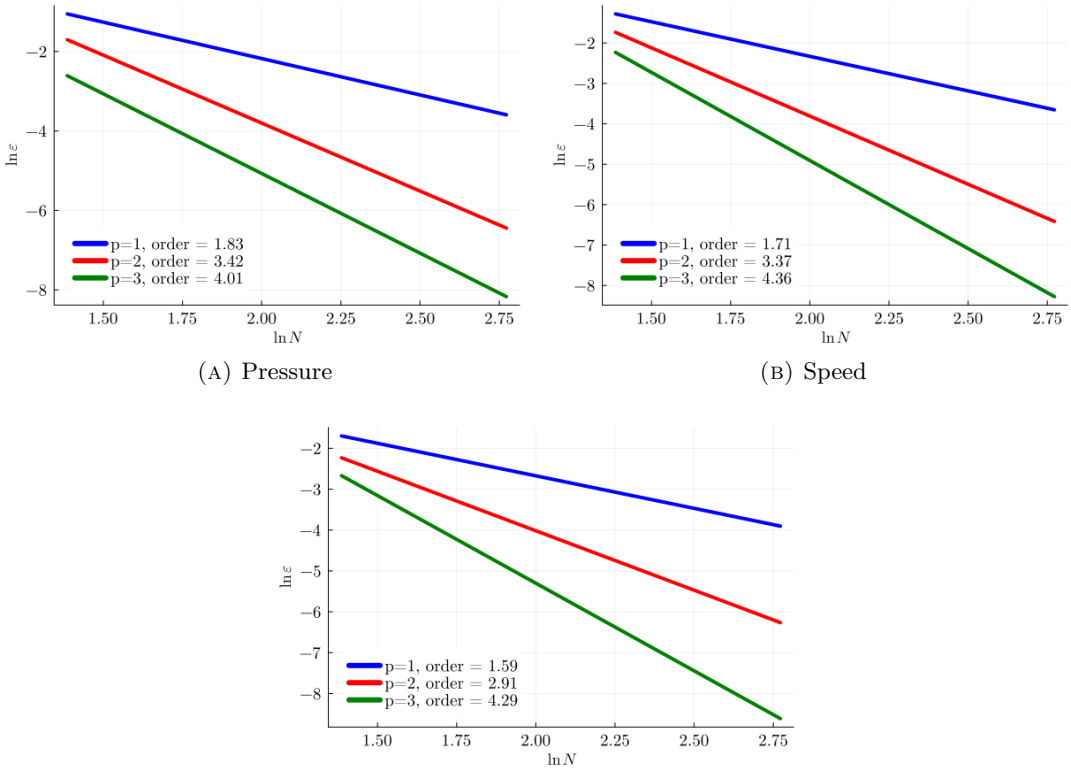

(A) Pressure

(B) Speed

(C) Angular Speed

FIGURE 4. Convergence order for the $2D$ numerical scheme

TABLE 3. Physical and Numerical parameters for the $2D$ stationary test case.

Parameter	Value	Unit	Description
E_0	3×10^6	kg cm^{-1} s^{-2}	Minimum Young modulus
E_1	3×10^8	kg cm^{-1} s^{-2}	Maximum Young modulus
h	0.05	cm	Thickness
ρ	1	kg cm^{-3}	Density
ξ	0.0		Poisson coefficient
R_0	0.5	cm	Maximum radius
R_1	0.3	cm	Minimum radius
ν	0.03	cm^2 s^{-1}	Kinematic viscosity
T	0.25	s	Final time
L	15	cm	Artery's length
cfl	0.5		Cfl
N_s	32		Number of elements in the s direction
N_θ	32		Number of elements in the θ direction
p	1		Polynomial degree

In Table 4, we give the physical and numerical parameters of the test case, also, we consider, for simplicity, the pressure at $r = R$ to be $P = \beta \frac{\sqrt{A}-\sqrt{A_0}}{A_0}$ even in the viscous case in Eq. (4). The following parameters are considered: $\beta = \frac{Eh\sqrt{\pi}}{\rho(1-\xi^2)}$, $A_0 = \pi R_0^2$. In the $2D$ case, these parameters

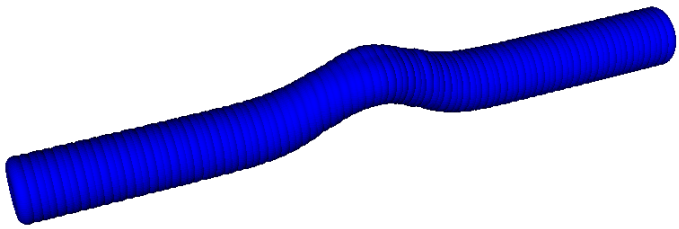

FIGURE 5. Artery Geometry

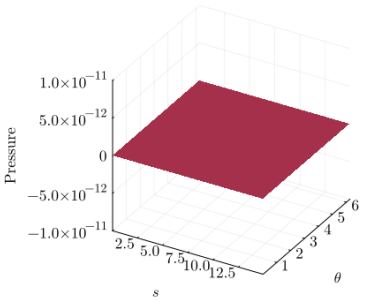

(A) Pressure

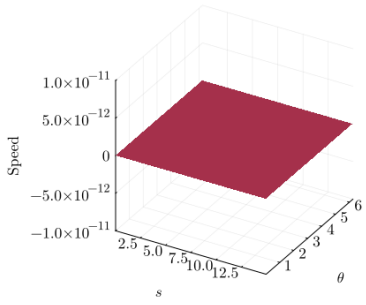

(B) Speed

FIGURE 6. Stationary solutions at $t = T$

are: $\beta = \frac{Eh}{\sqrt{2}\rho(1-\xi^2)}$, $A_0 = \frac{R_0^2}{2}$. We use the following curve $c(s) = (s, 0, 0)$ and we choose $\overrightarrow{n} = (0, 1, 0)$ by setting the curvature $\mathcal{C}(s) = 0$. To simulate a pressure wave entering into the domain, we use the following sinus-wave: $P(0,t) = \begin{cases} P_0 \sin(\pi \frac{t}{T_p}) & \text{if } t \le T_p, \\ 0 & \text{otherwise.} \end{cases}$ This lead to the following initial and boundary conditions,

$$\begin{aligned} &A(s,0) = A_0 && Q(s,0) = 0 \\ &A(0,t) = \left(\tfrac{A_0}{\beta} P(0,t) + \sqrt{A_0}\right)^2 && \partial_s Q(0,t) = 0 \\ &\partial_s A(15,t) = 0 && \partial_s Q(15,t) = 0 \end{aligned}$$

and for the $2D$, with $P(0,\theta,t) = \begin{cases} P_0 & \text{if } t \le T_p, \\ 0 & \text{otherwise} \end{cases}$ we set

$$\begin{aligned} &A(s,\theta,0) = A_0 && Q_\theta(s,\theta,0) = 0 && Q_s(s,\theta,0) = 0 \\ &A(0,\theta,t) = \left(\tfrac{A_0}{\beta} P(0,\theta,t) + \sqrt{A_0}\right)^2 && \partial_s Q_\theta(0,\theta,t) = 0 && \partial_s Q_s(0,\theta,t) = 0 \\ &\partial_s A(15,\theta,t) = 0 && \partial_s Q_\theta(15,\theta,t) = 0 && \partial_s Q_s(15,\theta,t) = 0. \end{aligned}$$

Periodic conditions are imposed on the direction θ. Figure 7 shows the geometry colored with the axial speed at time $t = \frac{T}{2}$.

In Figure 8, we compare the pressure obtained using the nonviscous 1D model in Eq. (3) with the data obtained from [19]. We also display the axial speed of the blood. We do the same in the viscous case (see equations (4)) in Figure 9 and in the 2D case (see equations (41)) in Figure 10.

TABLE 4. Physical and numerical parameters for TC1 (Realistic Pressure Wave in a straight artery).

Parameter	Value	Unit	Description
E	3×10^6	kg cm^{-1} s^{-2}	Young modulus
h	0.05	cm	Thickness
ρ	1	kg cm^{-3}	Density
ξ	0.0		Poisson coefficient
R_0	0.5	cm	Initial radius
ν	0 or 0.03	cm^2 s^{-1}	Kinematic viscosity
T	0.25	s	Final time
L	15	cm	Artery's length
P_0	2×10^4	kg cm^{-1} s^{-2}	Entering pressure amplitude
T_p	0.165	s	Pressure wave duration
σ	100		penalty parameter
cfl	0.5		Cfl
N	128		Number of elements for the 1D model
N_s	128		Number of elements in the s direction
N_θ	4		Number of elements in the θ direction
p	2		Polynomial degree

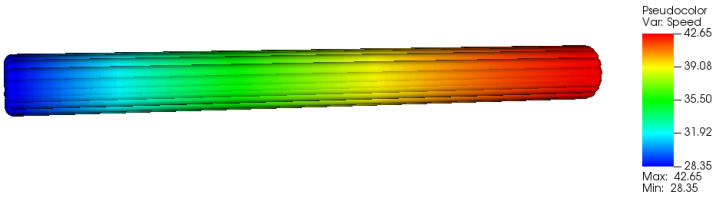

FIGURE 7. Artery geometry colored with axial speed at time $t = \frac{T}{2}$

Our numerical results are compared to those in [19] where the TGS (Taylor Galerkin Scheme) is used.

As expected, our numerical results ($2D$ and $1D$) are in a perfect agreement with those obtained in [19]. The results of the $1D$ and $2D$ models are almost identical because of the axisymmetry and curvaturless of the geometry. One can also remark that, in this case, the angular speed of the $2D$ model is almost zero everywhere (at least zero numerically) as shown in Figure 11. Moreover, one can see throughout this test case that the $1D$ viscous models provide mildly different numerical solutions compared to the inviscid models (TGS model and our $1D$ inviscid model).

4.4. **Addon of the 2D model and the limit of 1D model in the case of aneurysm.** In this test case, we compare the one-dimensional models $1D$ inviscid from Eq. (3) (solved by a DG method, see [**?**]) and $2D$ Eq. (41) solved by the DG method presented in section 3 in the case of a mild and a severe aneurysm to show the addon of the 2 model and the limit of the $1D$ model.

In Table 5, we present the physical and numerical parameters of the test case. We consider, for simplicity, the pressure at $r = R$ to be $P = \beta \frac{\sqrt{A}-\sqrt{A_0}}{A_0}$.

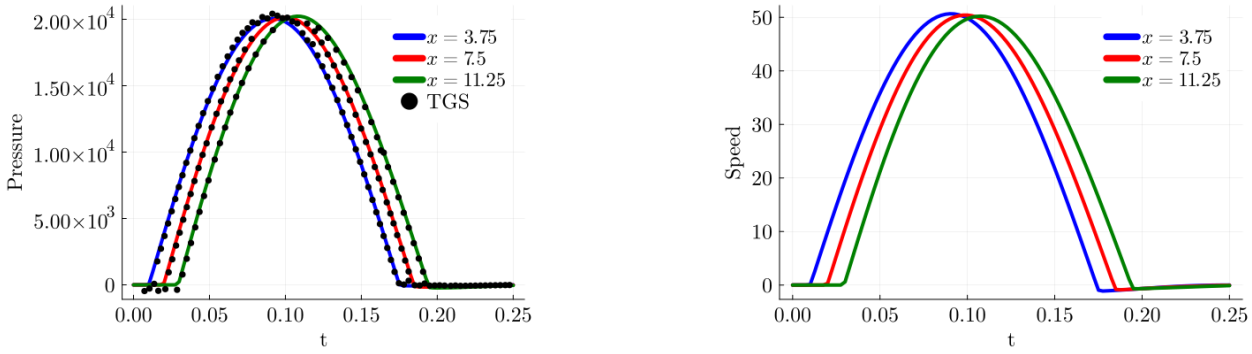

(A) Pressure (B) Speed

FIGURE 8. Pressure and Speed for the 1D nonviscous model and comparison with data obtained from [19]

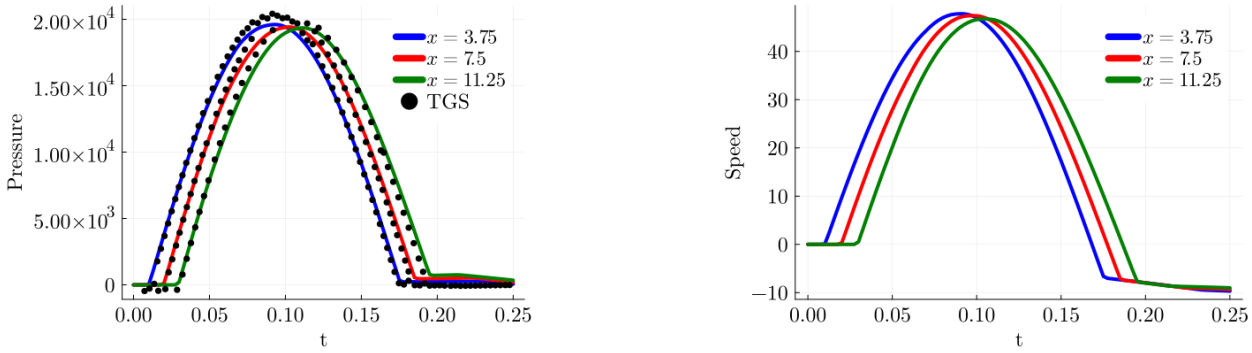

(A) Pressure (B) Speed

FIGURE 9. Pressure and Speed for the 1D viscous model and comparison with data obtained from [19]

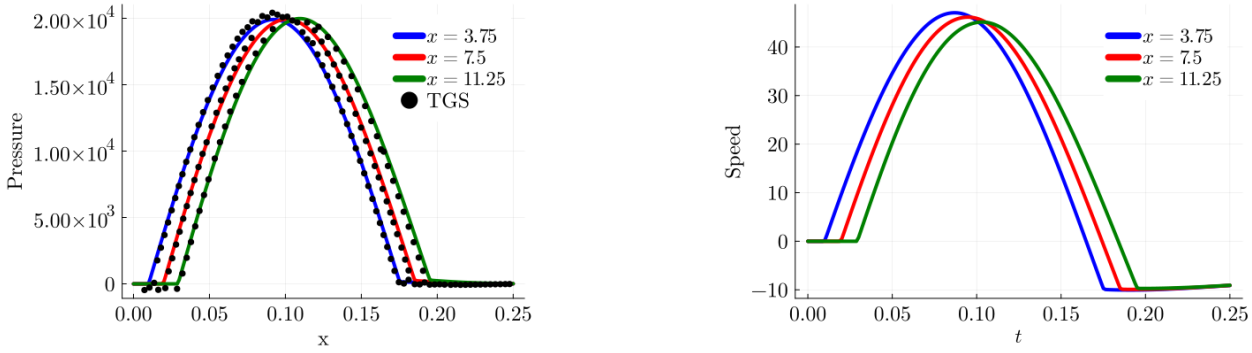

(A) Pressure (B) Speed

FIGURE 10. Pressure and Speed for the 2D model and comparison with data obtained from [19]

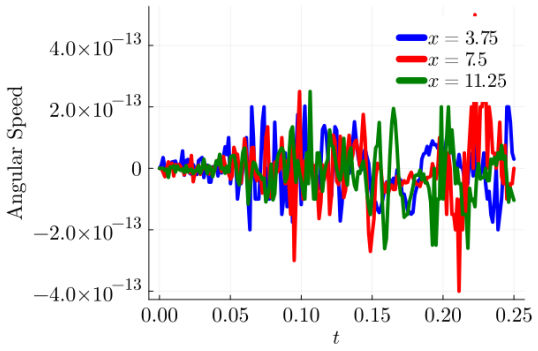

FIGURE 11. Angular Speed for the 2D model

We consider two different geometries mimicking a mild and a severe aneurysm. The initial geometry is given by : $A_0(s,\theta) = \frac{1}{2}\left(R_0 + (R_1 - R_0)e^{-(s-\frac{L}{2})^2}\left(e^{-\theta^2} + e^{-(\theta-2\pi)^2}\right)\right)^2$. The mild aneurysm is defined by $R_1 = 0.6$ and the severe one by $R_1 = 2$ (see Figure 12).

To compare the results issue from the $1D$ model to the $2D$ model, we integrate the numerical results from the $2D$ model over θ. The numerical results are presented in Figure 13 and Figure 14. We show the behavior in time of the pressure, the speed, and the maximum angular speed at the point $\frac{L}{2}$. As expected, in the case of a mild aneurysm, since the geometry of the artery is almost cylindrical, the results from the $1D$ and the $2D$ models are almost similar (see Figure 13). Whenever the aneurysm is severe, the geometry is no longer almost cylindrical, at least around the aneurysm, and important differences can be observed as shown in Figure 14. This is mainly because the angular speed is not zero in this case and can take large values. The $2D$ model can in practice compute more realistic solutions than the $1D$ one. The same observation holds at the control point $3L/4$.After the aneurysm, even if the geometry is cylindrical since the blood passed away a zone where the angular speed was not 0 (see Figure 15 and Figure 16), they are distinguishable difference between the $1D$ and the $2D$ models which confirms the limit of the $1D$ model. The more the amplitude of the maximum angular speed is, the more the difference observed between the $1D$ and the $2D$ models is.

5. Conclusion

In conclusion, we have developed a new two-dimensional model for blood flow simulations, for which we implemented a discontinuous Galerkin method. We have determined several mathematical and numerical properties, notably establishing that the scheme we constructed is well-balanced. Furthermore, through various test cases, we demonstrated the robustness of our method. Specifically, we compared 1D models with the 2D model in the context of both severe and mild aneurysms. This test case highlighted the limitations of 1D models.

References

[1] K. Azer and C. S. Peskin. A one-dimensional model of blood flow in arteries with friction and convection based on the womersley velocity profile. *Cardiovascular Engineering*, 7:51–73, 2007.

[2] F. Berntsson, A. Ghosh, V. Kozlov, and S. Nazarov. A one dimensional model of blood flow through a curvilinear artery. *Applied Mathematical Modelling*, 63:633–643, 2018.

[3] S. Čanić. Blood flow through compliant vessels after endovascular repair: wall deformations induced by the discontinuous wall properties. *Computing and visualization in science*, 4:147–155, 2002.

[4] S. Čanić and E. H. Kim. Mathematical analysis of the quasilinear effects in a hyperbolic model blood flow through compliant axi-symmetric vessels. *Mathematical Methods in the Applied Sciences*, 26(14):1161–1186, 2003.

TABLE 5. Physical and numerical parameters for TC4 (Addon of the 2D model over the 1D model in complex geometry).

Parameter	Value	Unit	Description
E	3×10^6	kg cm^{-1} s^{-2}	Young modulus
h	0.1	cm	Thickness
ρ	1	kg cm^{-3}	Density
ξ	0.0		Poisson coefficient
R_0	0.5	cm	Initial radius
R_1	2.0	cm	Secondary radius
ν	0 or 0.03	cm^2 s^{-1}	Kinematic viscosity
T	0.03	s	Final time
L	10	cm	Artery's length
P_0	13 332	kg cm^{-1} s^{-2}	Entering pressure amplitude
T_p	0.005	s	Pressure wave duration
σ	1		Penalty parameter
cfl	0.5		Cfl
N	32		Number of elements for the 1D model
N_s	32		Number of elements in the s direction
N_θ	32		Number of elements in the θ direction
p	2		Polynomial degree

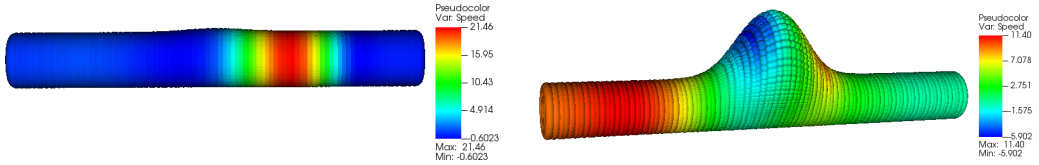

(A) Case of the mild aneurysm with $R_1 = 0.6$

(B) Case of the severe aneurysm with $R_1 = 2$

FIGURE 12. Initial geometry and Speed for the $2D$ at $t = \frac{T}{2}$

[5] J.-B. Clément. *Numerical simulation of flows in unsaturated porous media by an adaptive discontinuous Galerkin method: application to sandy beaches*. PhD thesis, Université de Toulon, 2021.

[6] B. Cockburn. Discontinuous galerkin methods. *ZAMM-Journal of Applied Mathematics and Mechanics/Zeitschrift für Angewandte Mathematik und Mechanik: Applied Mathematics and Mechanics*, 83(11):731–754, 2003.

[7] M. A. Debyaoui and M. Ersoy. A generalised serre-green-naghdi equations for variable rectangular open channel hydraulics and its finite volume approximation. In *Recent Advances in Numerical Methods for Hyperbolic PDE Systems: NumHyp 2019*, pages 251–268. Springer, 2021.

[8] M. Ersoy. Dimension reduction for incompressible pipe and open channel flow including friction. In *Conference Applications of Mathematics 2015, in honor of the 90th birthday of Ivo Babuška and 85th birthday of Milan Práger and Emil Vitásek* , pages 17–33, Institute of Mathematics CAS, Prague, France, Nov. 2015. J. Brandts and S. Korotov and M. Křížek and K. Segeth and J. Šístek and T. Vejchodský.

[9] M. Ersoy. Dimension reduction for compressible pipe flows including friction. *Asymptotic Analysis*, 98(3):237–255, 2016.

[10] M. Ersoy, O. Lakkis, and P. Townsend. A saint-venant model for overland flows with precipitation and recharge. *Mathematical and Computational Applications*, 26(1):1, 2020.

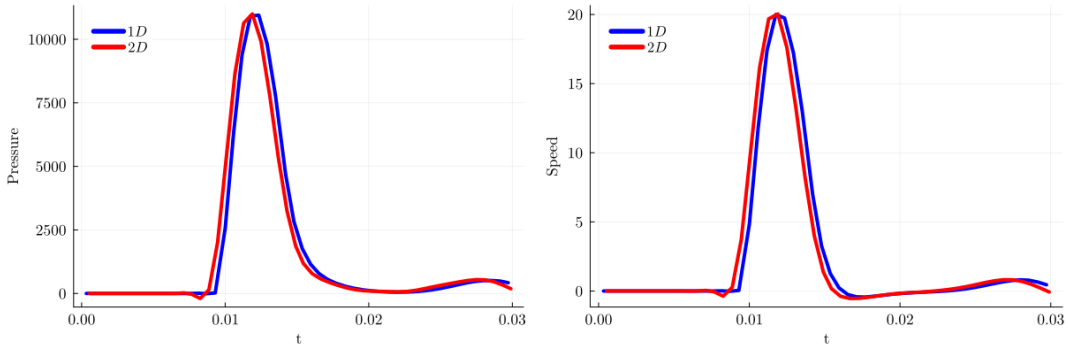

(A) Pressure (B) Speed

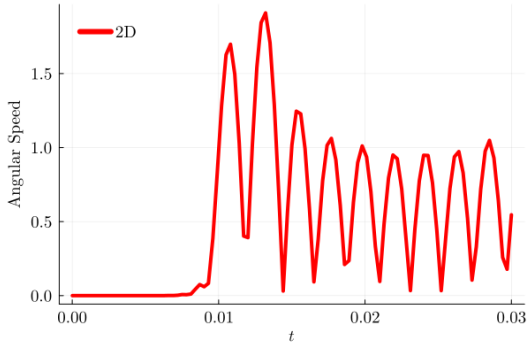

(C) Angular Speed

FIGURE 13. Pressure, axial speed and maximum angular speed for the 2D and 1D model at the point $\frac{L}{2}$ for $R_1 = 0.6$.

[11] L. Formaggia, J.-F. Gerbeau, F. Nobile, and A. Quarteroni. On the coupling of 3d and 1d navier–stokes equations for flow problems in compliant vessels. *Computer methods in applied mechanics and engineering*, 191(6-7):561–582, 2001.

[12] L. Formaggia, F. Nobile, and A. Quarteroni. A one dimensional model for blood flow: application to vascular prosthesis. In *Mathematical Modeling and Numerical Simulation in Continuum Mechanics: Proceedings of the International Symposium on Mathematical Modeling and Numerical Simulation in Continuum Mechanics, September 29–October 3, 2000 Yamaguchi, Japan*, pages 137–153. Springer, 2002.

[13] Y.-c. Fung. *Biomechanics: mechanical properties of living tissues*. Springer Science & Business Media, 2013.

[14] J.-F. Gerbeau and B. Perthame. *Derivation of viscous Saint-Venant system for laminar shallow water; numerical validation*. PhD thesis, INRIA, 2000.

[15] L. Grinberg. Modeling blood flow circulation in intracranial arterial networks: a comparative 3d/1d simulation study. *Annals of biomedical engineering*, 39(1):297–309, July 2010.

[16] Y. Huo and G. S. Kassab. A hybrid one-dimensional/womersley model of pulsatile blood flow in the entire coronary arterial tree. *American Journal of Physiology-Heart and Circulatory Physiology*, 292(6):H2623–H2633, 2007.

[17] G. V. Krivovichev. Computational analysis of one-dimensional models for simulation of blood flow in vascular networks. *Journal of Computational Science*, 62:101705, 2022.

[18] P. Nardinocchi, G. Pontrelli, and L. Teresi. A one-dimensional model for blood flow in prestressed vessels. *European Journal of Mechanics-A/Solids*, 24(1):23–33, 2005.

[19] A. Quarteroni and L. Formaggia. Mathematical modelling and numerical simulation of the cardiovascular system. *Handbook of numerical analysis*, 12:3–127, 2004.

[20] J. Ventre. *Reduced-order models for blood flow in the large arteries: applications to cardiovascular pathologies*. PhD thesis, Sorbonne Université, 2020.

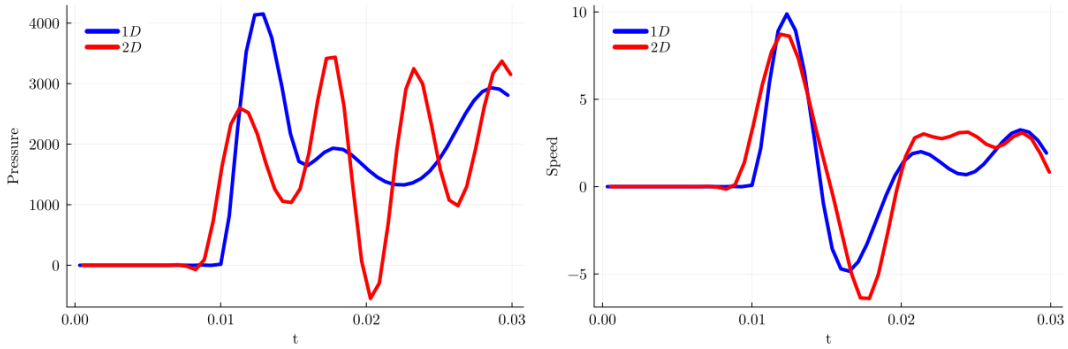

(A) Pressure (B) Speed

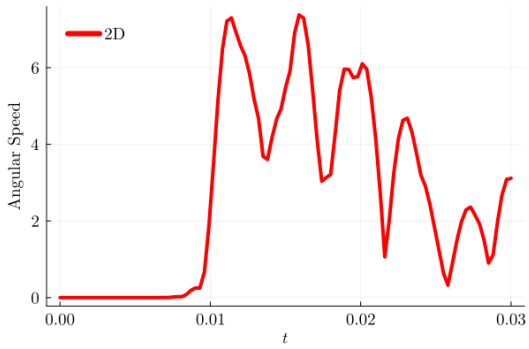

(C) Angular Speed

FIGURE 14. Pressure and Speed for the 2D and 1D model at the point $\frac{L}{2}$ for $R_1 = 2$.

INSTITUT DE MATHÉMATIQUES DE TOULON (IMATH), UNIVERSITÉ DE TOULON, LA GARDE, FRANCE
HOSPICES CIVILS DE LYON, FRANCE

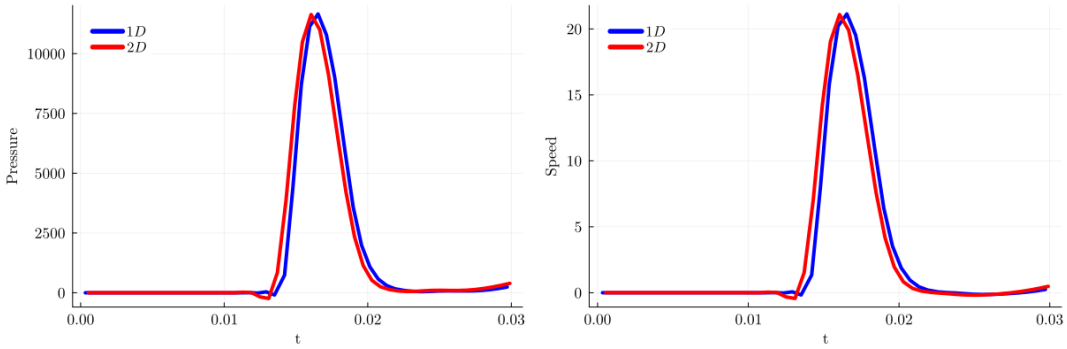

(A) Pressure (B) Speed

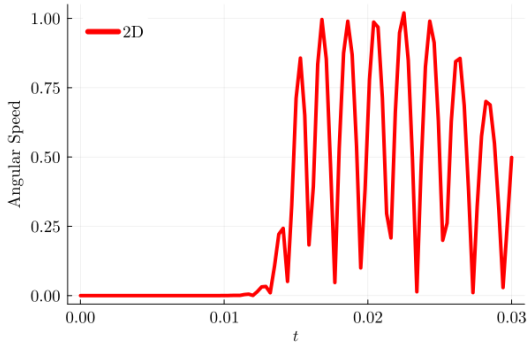

(C) Angular Speed

FIGURE 15. Pressure, axial speed and maximum angular speed for the 2D and 1D model at the point $\frac{3L}{4}$ for $R_1 = 0.6$

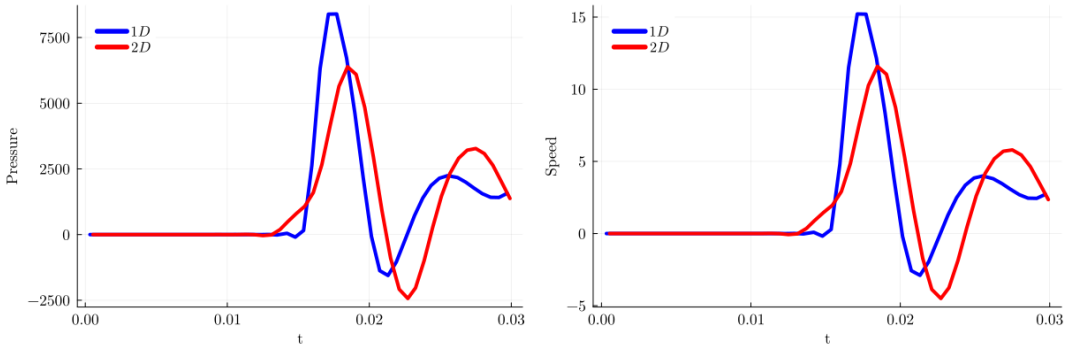

(A) Pressure

(B) Speed

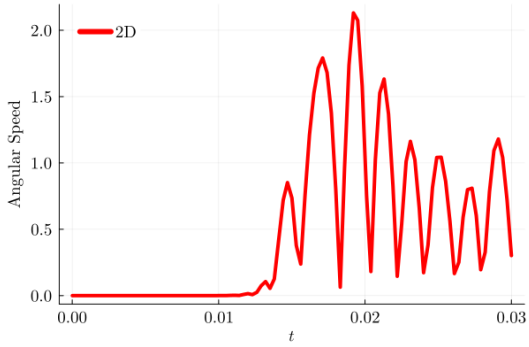

(C) Angular Speed

FIGURE 16. Pressure, axial speed and maximum angular speed for the 2D and 1D model at the point $\frac{3L}{4}$ for $R_1 = 2$.